017 KORTRAPPORT/BRIEF REPORT SERIES
NORSK POLARINSTITUTT 2010

Report from the international workshop:

Black carbon in snow – sampling, albedo effects and climate impact

Tromsø, Norway, 13–14 August 2009

Editors:
Christina A. Pedersen, Terje K. Berntsen, Sebastian Gerland, and Stephen G. Warren

Kortrapport/Brief Report Series nr 17.

Report from the international workshop:

Black carbon in snow – sampling, albedo effects and climate impact

Tromsø, Norway, 13–14 August 2009

Editors:
Christina A. Pedersen, Terje K. Berntsen, Sebastian Gerland, and Stephen G. Warren

Norsk Polarinstitutt er Norges sentralinstitusjon for kartlegging, miljøovervåking og forvaltningsrettet forskning i Arktis og Antarktis. Instituttet er faglig og strategisk rådgiver i miljøvernsaker i disse områdene og har forvaltningsmyndighet i norsk del av Antarktis.

The Norwegian Polar Institute is Norway's main institution for research, monitoring and topographic mapping in Norwegian polar regions. The Institute also advises Norwegian authorities on matters concerning polar environmental management.

Address
Norwegian Polar Institute
Polar Environmental Centre
NO-9296 Tromsø
Norway
post@npolar.no
www.npolar.no

Editors:
Christina A. Pedersen, Norwegian Polar Institute, Tromsø, Norway
Terje K. Berntsen, University of Oslo, Oslo, Norway
Sebastian Gerland, Norwegian Polar Institute, Tromsø, Norway
Stephen G. Warren, University of Washington, Seattle, USA

Photo, cover: Christina A. Pedersen, NPI
Printed: May 2010
ISBN: 978-82-7666-270-2
ISSN 1504-3215

Table of contents

Back row from left: Gunnar Myhre, Kostas Eleftheriadis, Øyvind Seland, Sebastian Gerland, Sarah Doherty, Borgar Aamaas, Terje K. Berntsen, Ragnhild B. Skeie, Christina A. Pedersen, Lars Otto Reiersen, and Joe McConnell. Middle row from left: Nicolas Bellouin, Charlie Zender, Dean Hegg, Ross Edwards, Stephen G. Warren, Stephen R. Hudson, Kim Holmén, and Mark Flanner. Front row from left: Rune Solberg, Dorothy Koch, Marianne Lund, Benjamin DeAngelo, Tami Bond, Sanja Forsström, Wiley Bogren, and Thomas C. Grenfell. Not present when the picture was taken: Nalân Koç, Birgit Njåstad, and Stian Solbø. Photo: A. E. Tønset, Norwegian Polar Institute.

Introduction

In the framework of the project *Measurements of Black carbon aerosols in arctic snow – interpretation of effect on snow reflectance*, a collaborative project between CICERO, Norwegian Polar Institute, University of Oslo, Stockholm University and University of Washington, and funded by *the Research Council of Norway*, an international workshop on *Black carbon in snow – sampling, albedo effects and climate impact* was held in Tromsø 13–14 August 2009. Scientists working with applied climate research (observations, processes) and modelers were brought together to discuss the overall climate impacts of emissions of Black carbon aerosols.

Black carbon (BC or soot) consists of small particles emitted by fossil fuel and biomass combustions. The sources are both natural (biomass burning including forest fires) and from human activities (industry, transportation and household). These particles are black and extremely efficient absorbers of solar radiation and have a significant direct effect on climate. In addition, the absorbing BC particles may affect the clouds and act on the climate through indirect effects. Most of the larger particles stay close to the sources, mainly at lower latitudes, but the smaller particles can be transported over large distances to the Arctic where some of the BC particles are deposited on the snow and ice. The effect of BC on snow albedo depends on the vertical variation of snow grain size as well as the thickness distribution of the snowpack. For example, 40 parts per billion of soot can reduce the albedo by 1–3% (depending on snow grain size). The climate effect of BC particles transported to the Arctic is potentially large because of the sensitivity of surface albedo changes to snow and ice albedo feedback mechanisms.

The two day workshop aimed at discussing new findings and identifying processes where more research is needed. The workshop had sufficient time for presentations, grouped in six sessions; Black carbon in arctic snow, Black carbon in Norway, Effects of Black carbon on the albedo and remote sensing, Black carbon sources and atmospheric transport, Climate modeling and Mitigation. The second day also consisted of plenum discussions in two working groups; *Modeling* and *Measurements*.

This report contains the workshop program, extended abstracts from 16 of the 23 presentations, and notes from the working groups. The power point presentations from the meeting can be downloaded at: ftp://ftp.npolar.no/Out/Xtina/BC_workshop_Tromso_aug2009/

Christina A. Pedersen
christina.pedersen@npolar.no
Norwegian Polar Institute

Terje K. Berntsen
t.k.berntsen@geo.uio.no
University of Oslo

Sebastian Gerland
gerland@npolar.no
Norwegian Polar Institute

Stephen G. Warren
sgw@atmos.washington.edu
University of Washington

Workshop program

13 August 2009
09:00–09:15: Welcome
09:15–10:35: Session 1
10:35–11:00: Coffee break
11:00–12:20: Session 2
12:20–13:30: Lunch
13:30–14:50: Session 3
14:50–15:30: Coffee break and posters
15:30–16:50: Session 4

14 August 2009
08:00–09:20: Session 5
09:20–09:40: Coffee break
09:40–10:40: Session 6
10:45–10:50: Introduction to working groups
10:50–12:50: Working groups
12:50–13.50: Lunch
13:50–14:50: Report from working groups
14:50–15:05: Coffee break
15:05–15:45: Discussions, closure

Session 1. Black carbon in arctic snow
09:15–09:35: T. C. Grenfell – Spectral absorption by particulate impurities determined by photometric analysis of filters
09:35–09:55: S. Doherty – A survey of BC concentrations in arctic snow, and comparisons with model values
09:55–10:15: J. McConnell – Reconstructing Black carbon and other aerosols histories from ice cores: Developing an arctic array
10:15–10:35: R. Edwards – Uncertainties in the analysis of BC in snow: Are we missing something?

Session 2. Black carbon in Norway
11:00–11:20 K.Eleftheriadis – Lessons learned from 10 years monitoring of Black carbon aerosol at Ny-Ålesund, Svalbard – Concentration levels, sources and optical properties
11:20–11:40: S. Forsström – Elemental carbon distribution in Svalbard snow
11:40–12:00: B. Aamaas – Elemental carbon in snow from Norwegian settlements in Svalbard
12:00–12:20: J. Ström – On the spatial and temporal variation of Elemental carbon in snow

Session 3. Effects of Black carbon on albedo and remote sensing
13:30–13:50: C. A. Pedersen – The effect of Black carbon on spectral snow albedo derived from *in-situ* measurements
13:50–14:10: S. G. Warren – Relating BC content to albedo reduction
14:10–14:30: C. Zender – Darkening of soot-doped natural snow: Measurements and model
14:30–14:50: R. Solberg – Remote sensing of Black carbon at snow and glacier ice surfaces – first results of a modeling approach

Session 4. Black carbon sources and atmospheric transport

15:30–15:50: T. Bond – Black carbon sources and co-emitted pollutants by latitude and region
15:50–16:10: D. Hegg – Seasonal variability in the sources of Black carbon in arctic snow
16:10–16:30: M. Lund – Parameterization of BC aging in the Oslo CTM2 and the effect on transport to the Arctic
16:30–16:50: R. B. Skeie – Black carbon in the atmosphere and deposition on snow, last 130 years

Session 5. Climate modeling

08:00–08:20: N. Bellouin – Climate response and efficacy of snow albedo forcing in the HadGEM2-AML climate model
08:20–08:40: M. Flanner – Springtime solar heating and albedo feedback from carbonaceous particles
08:40–09:00: D. Koch – BC-albedo effects on climate during the 20th century in the GISS model
09:00–09:20: Ø. Seland – Deposition and radiative effects in the Arctic from Black carbon modeled in the Norwegian Earth System Model.

Session 6. Mitigation

09:40–10:00: B. DeAngelo – Task force on short lived climate forcers under the Arctic Council
10:00–10:20: G. Myhre – Global temperature effect from Black carbon reductions
10:20–10:40: T. K. Berntsen – Costs and global impacts of BC abatement strategies

Posters

1) J. Ström: Specific absorption coefficient, Seasonal variation of OC and EC: Observations from the Zeppelin station, Ny-Ålesund, Svalbard.
2) W. Bogren: Initial results in spatial variability and albedo effects in Ny-Ålesund

Extended Abstracts

Session 1. Black carbon in arctic snow

Spectral absorption by particulate impurities in snow determined by photometric analysis of filters

T. C. Grenfell[1], S. J. Doherty[1], and A. D. Clarke[2]
[1]Department of Atmospheric Science, University of Washington, Seattle, Washington, USA;
[2]Dept. of Oceanography, University of Hawai'i, Honolulu, Hawaii USA

Our work was motivated by the 1983–84 survey of soot in arctic snow by Clarke and Noone (1985). That study showed the significance of understanding levels of Black carbon soot (BC) and other light-absorbing particulates in snow and their influence on the albedo and other optical properties of the snow cover. Their survey included an array of sites across the Western Arctic north of 65^{o} N latitude but did not include the Eastern Arctic.

Our objective has been to resurvey the original area and extend the observations around the entire Arctic Basin. The IPY program allowed us to carry out cooperative experiments with Norwegian, Russian, and Canadian research groups to achieve our goals. Among the various methods available for measuring light-absorbing particulates in snow, we chose to continue to use the filter absorption method of Clarke and Noone (1985). The principal advantages of this technique are (a) that it measures light absorption directly and the result is closely related to the actual absorption of sunlight in the snow and (b) that processing and filtering of the samples can be carried out in remote locations and it is not necessary to transport large samples of snow back to our laboratory in Seattle. The filtration apparatus has been set up in laboratories, hotel rooms, and on one occasion in a tent. The only electric power required is that needed to run a small microwave oven used to melt the samples quickly. The loaded filters are dried and stored in transparent plastic Analyslide® cases. A by-eye comparison against a set of standard filters is carried out on site to estimate the filter loading in μgC/cm^2, which combined with the volume of water filtered gives the concentration of absorbing particulates in the snow. Sixty-ml samples of the filtered water are also collected for chemical analysis for source attribution studies (see abstract by D. Hegg in this volume). Since the visual appearance of the loaded filters can vary considerably depending on ambient illumination, the by-eye estimates are only the first stage in the analysis. This has motivated the use of the integrating sandwich technique (Clarke, 1982) described below.

To improve the accuracy in determining filter loading, we have designed and constructed a spectrophotometer system making use of modern improvements in optical technology. The new instrument is called an Integrating Sphere Sandwich (ISSW) Spectrophotometer. It makes use of a 50 mm Spectralon® integrating sphere in conjunction with a newly designed sample cell. The integrating sphere projects nearly isotropic incident radiation onto the filter. This assembly is connected by optical fiber to an Ocean Optics Red Tide USB spectrophotometer operated using a standard laptop computer. The spectrophotometer runs on 5V DC and has very low noise and negligible drift when allowed to equilibrate at ambient room temperature. Illumination is provided by a 150W quartz halogen lamp in a Dolan-Jenner regulated power supply via a second optical fiber. The light source is stable to better than 0.4% over intervals of several hours.

The spectrophotometer uses a high sensitivity CCD photosensor and has a spectral resolution of about 2 nm. The system is designed to record over a wavelength range from ~410 nm to ~750 nm. The sensitivity is limited at short wavelengths by the detector sensitivity and at long wavelengths by a heat-absorbing filter built into the light source. This wavelength range closely approximates the range over which naturally occurring background levels of BC and other absorbing particulates have a significant effect on the optical properties of snow. At

longer wavelengths, the snow itself becomes the dominant absorber (e.g. Warren and Wiscombe, 1980).

The sample cell makes use of a stainless steel weight that is raised manually to insert the filter sample. When closed the weight provides identical compression for all samples. The weight is the only moving part in the system. All other elements are fixed, eliminating noise due to variations in alignment.

An integrating sandwich configuration is used to remove effects of scattering by particles on filter. Scattering by such particles including those that are weakly absorbing or non-absorbing can produce light loss that is incorrectly interpreted as absorption, resulting in overestimation of the BC loading. The integrating sandwich is achieved by mounting a strong diffuser on the compression weight providing strong scattering and a fully diffuse radiation field around the filter via multiple reflection of the light. This overwhelms the effects of scattering by materials on the filter, leaving absorption as the detected signal. Both the integrating sphere and the diffuser have backscatter efficiencies of 98% over the full wavelength range.

The system is calibrated relative to a set of standard filters with various loadings of Monarch-71 (M71) soot, whose mass absorption efficiency (β_a) is ~6 m^2/g. The calibration curve of absorption, $\tau = -\ln[I(\text{loaded filter})/I(\text{bare filter})]$, versus loading (L) in $\mu gBC/cm^2$ is slightly non-linear, a characteristic of the integrating sandwich technique. We have fitted the curve to a function of the form $L = A\,\tau + B\,\tau^3$. The coefficients A and B are functions of wavelength.

An extensive analysis of the errors and uncertainties of the system has been carried out. A set of 14 runs carried out over a period of two weeks determined that the system calibration is extremely stable, showing a 2-standard deviation variation of 5%. Measurements of noise versus sample loading showed that above a threshold of about 0.5 $\mu gC/cm^2$ the accuracy is 3–4% as compared with an estimated factor of 2 using by-eye comparison.

In general the color of loaded filters shows the presence of other material in addition to BC, such as windborne dust or dirt. We make use of the spectral dependence of absorption to determine the integrated relative absorption of BC and non-BC material. As a first approximation, we assume that all the absorption in the 650 to 700 nm band is due purely to BC and gives the BC loading of the sample. Then we compare the known wavelength dependence absorption of M71 soot from the standard samples to the observed wavelength dependence of absorption for a given sample. If non-BC material is present, the latter shows an excess at shorter wavelengths. We then weight the two curves by the incident solar spectrum to calculate the integrated solar energy absorption in both cases, and the ratio gives the fraction of total absorption due to BC. Typically this shows that 15–30% of the absorption is due to non-BC material. Because non-BC material does absorb to some extent between 650 and 700 nm, this estimate is a lower limit for non-BC and an upper limit for BC. We are presently investigating the absorption spectra of non-BC materials to refine our estimates.

A comparison of results from by-eye estimates to results from the ISSW spectrophotometer confirmed the estimated factor-of-two uncertainty in the by-eye results but showed negligible bias over more than two orders of magnitude of loading. This provides support for our previous estimates made before the ISSW instrument was available. We are presently processing all our samples with the new instrument.

Our presentation contains three supplementary slides. The first slide shows that Mie calculations using log normal size distributions with reasonable values of mass mean

diameter closely reproduce the observed wavelength dependence of absorption observed for our standard filters made using M71 soot.

The second slide discusses four additional uncertainties associated with soot sampling not mentioned above. (1) Multiple measurements of a given filter, re-centering them in ISSW observing cell each time. This produces errors less than 4%. (2) Occasional errors on the order of 10% can be caused by slippage of the filter, in which case the sample is reprocessed with more careful positioning. Moving a filter around in ISSW intentionally to look at filter homogeneity appears to explain the cases for these large errors, although some of the filters are exposed non-uniformly and are therefore assigned lower weight. (3) Undercatch by the 0.4-μm nuclepore filters due to the presence of small BC particles is quite variable, ranging from 0 to 20%. We have not observed significantly larger values of undercatch for natural samples, indicating that amounts we might be missing do not obscure or mask the actual spatial or interannual variations in soot loading.(4) Are our sampling sites representative? Did we get far enough away from local sources to obtain background levels? We believe we are able to select the proper background values based on looking at the spatial distribution of values at differing distances from local population areas, studying statistical wind patterns to determine how likely local contamination might have reached a given site, and looking at our full field of samples for anomalous readings.

Finally we urge all groups reporting soot loadings in snow or ice to report also the appropriate absorption coefficients to include in radiative transfer calculations. This will help to avoid errors and ambiguities in applying these results to climate models.

Our conclusions are as follows: (1) The system stability is better than 1%; (2) Precision relative to ADC standards is 3–4% for loadings greater than about 0.5 $\mu gC/cm^2$; (3) We can distinguish BC absorption from non-BC absorption from relative spectral shapes of the energy absorption curves with an accuracy that will depend on our knowledge of the spectral absorption curves of the non-BC components; (4) By-eye estimates are consistent with new ISSW results. A continuing outstanding question is what is the appropriate value to use for the mass absorption efficiency, β_a? In particular, what is the difference between β_a for BC on filters versus in snow and ice? If the BC is inside the snow particles its absorption efficiency can be twice as high as if the same material is outside the ice.
Please refer to the extended abstract of S. J. Doherty (in this report) for results obtained with this instrument and to the extended abstract of S. G. Warren (in this report) for experimental studies relating to the calibration of our method. General details for our project are available on our web site at http://www.atmos.washington.edu/sootinsnow/.

References

Clarke, A. D. Integrating sandwich: a new method of measurement of the light absorption coefficient for atmospheric particles, *Applied Optics, 21*, 3011–3020, 1982.

Clarke, A. D., and K. J. Noone. Soot in the arctic snowpack: A cause for perturbations in radiative transfer, *Atmospheric Environment, 19*, 2045–2053, 1985.

Warren, S. G., and W. J. Wiscombe. A model for the spectral albedo of snow, II: Snow containing atmospheric aerosols, *J. Atmos. Sci., 37*, 2734–2745, 1980.

A survey of BC concentrations in arctic snow

S. Doherty[1], S. Warren[2], T. Grenfell[2], and A. Clarke[3]
[1]Institute for the Study of the Atmosphere and Ocean (JISAO), University of Washington, Seattle, Washington USA; [2]Deptartment of Atmospheric Science, University of Washington, Seattle, Washington USA; [3]Deptartment of Oceanography, University of Hawaii, Honolulu, Hawaii USA

Here we report concentrations of Black carbon (BC) in arctic snow as made with a photometric measurement technique described by Grenfell et al. (this report). As noted therein our study is an extension to earlier measurements of a smaller set of arctic snow samples (Clarke and Noone, 1985). In sum: Snow is collected, melted and drawn through 0.4 μm nuclepore filters. Light absorption is measured with a photometer (420–750 nm) as a decrease in transmission of light through the filter. Synthetic soot calibration standards are used to convert the measured transmission loss to soot loading (μgC/cm^2) on the filter. Knowledge of the volume of water filtered allows us to calculate the quantity of soot present in the snow water (ngC/gm). The wavelength-dependence of the loss in transmittance (absorption) can be used to approximate the relative contributions of soot and non-soot constituents (e.g. soil dust, "brown" carbon) to light absorption by aerosol in the snow. This is done by assuming that the wavelength-dependence of absorption for soot follows λ^{-1}, as indicated in a number of studies (e.g. Kirchstetter et al., 2004; Bergstrom et al., 2007; Sun et al., 2007).

There are several aspects of our measurement technique which may lead to biases in our results. First, we use calibration standards of synthetic soot with a certain mass absorption efficiency, so the derived loading is an equivalent BC mass which will equal the mass of the BC in the snow if the mass absorption efficiency of the soot in the snow matches that of the calibration standard synthetic soot (in this case 6 m^2/gm). Second, our process assumes the all absorption by the aerosols in the 650–700 nm wavelength band is due to BC. Therefore, our derived BC mass is a maximum value. Following on this, the derived fraction of absorption due to non-BC constituents ($f_{abs,non\text{-}BC}$) is a minimum. Finally, the data presented here have not yet been corrected for under-catch of aerosols by the nuclepore filters. Tests indicate that under-catch is on the order of ~10% (range: ~0–20%, depending on the sample tested).

The samples analyzed were collected from sites across high northern latitudes, and we have grouped the data by region and sample collection date. Of primary concern is the concentration of BC in the surface snow in springtime, as this is when there is simultaneously sunlight incident on the snow and a maximum in snow cover, and thereby the largest potential radiative forcing. Therefore, with the exception of Greenland (sampled in July), all sites were sampled in the April to May timeframe. In all cases an effort was made to sample snow from areas sufficiently far away from local sources as to be regionally representative.

The median concentrations of BC in the surface snow at the sites sampled is: central Canadian transect, 2007: 14 ng/g; Canadian Arctic survey, 2009: 10 ng/g; Barrow, Alaska, 2008: 11 ng/g; Western Russia, 2007: 19 ng/g; Eastern Russia, 2008: 45 ng/g; Tromso, Norway, 2008: 29 ng/g; Ny Alesund, Svalbard, Norway, 2007: 14 ng/g; Greenland, 2007: 4 ng/g; Greenland, 2008: 1 ng/g; North Pole region, 2008: 6 ng/g. However, there was a great deal of variation in BC concentrations in some regions, most notably across Eastern and Western Russia, central Canada, and on Svalbard. Some of this may be due to inaccurately

removing the influence of non-BC constituents; however, we expect that a large amount of the observed variability is real. In contrast, the observed concentrations were very consistent across different locations within the Canadian Arctic and on the Greenland ice sheet (i.e. away from the low-elevation coastline). Using the range of concentrations given above and the calculations of soot mass fraction vs. change in snow albedo given by Warren and Wiscombe (1985), we get a range of change in albedo from ~0.001 (Greenland) to ~0.035 (Eastern Russia, if the snow has the typical radius for aged snow of 1mm), or a change in albedo of <0.1–4%.

Of interest is the source of the BC in the snow. To a first order, it is expected that fossil fuel sources will produce a relatively high ratio of Black carbon (soot) to Organic carbon and that biomass burning will produce a relatively lower fraction of Black carbon to Organic carbon. It is also expected that light-absorbing Organic carbon will have a steeper spectral absorption "fingerprint" (i.e. be more brown, so λ^{-x} where x>1) than will BC (e.g. Kirchstetter et al., 2004; Sun et al., 2007). Thus, we can use our derived fraction of absorption due to non-BC constituents ($f_{abs,non\text{-}BC}$) as an indicator of whether the light-absorbing aerosol in the snow came predominantly from fossil fuel burning or biomass burning – to the extent that we have avoided including soil dust in our snow sample. Unfortunately, the wavelength-dependence of soil dust is also expected to follow λ^{-x} where x>1, and the value of "x" is not sufficiently well know for the large range of airborne soil dust and organics in order to distinguish the two. Nonetheless, it is interesting to note that the samples appear to fall fairly neatly into two ranges of $f_{abs,non\text{-}BC.}$ All of Western Russia, two of the sites in Eastern Russia, Ny Alesund, and Tromso all have values ~15–20%, whereas most of the Eastern Russian sites, Canada, Barrow, Greenland and the North Pole area samples all had values ~25–30%. These are consistent with the expected sources of BC to these areas, in particular for Ny Alesund and Tromso (industry in eastern Europe and western Siberia) and for Canada, Greenland and Barrow (biomass burning from northern Canada and Greenland). The mix of results in Russia likely reflects that there are both heavy industrial sources and a large amount of biomass burning in Russia. Notably, the one site we sampled that we know was heavily influenced by local industrial sources has the lowest measured $f_{abs,non\text{-}BC}$: 10%. This is a good indication that our analysis is sound in principle.

In addition to the surface snow samples, in some locations we collected vertical profiles of snow samples. These can be used to quantify the seasonal evolution of BC in the snow. In addition, an open question is whether the BC in the snow is sufficiently hydrophobic that when the snow melts it is left at the surface. This is potentially important in that it would produce a positive feedback: the presence of soot in the snow reduces its albedo, leading to earlier melt; the melt process increases the concentration of BC on the snow surface, further lowering the albedo and accelerating melt, etc. (Flanner et al., 2007). Vertical snow samples taken during the melt season help confirm and constrain the extent to which this process is at play. Finally, in addition to looking at vertical variations in BC concentrations we can look at vertical variations in $f_{abs,non\text{-}BC,}$ which provides an indication of whether the source of light-absorbing aerosol in the snow changes through the winter/spring season.

We have vertical profiles of snow samples from the Canadian Arctic, Russia, Greenland and Tromso. For Greenland and Tromso we have data during the melt season. (*Sample from Tromso, credit Sanja Forsstrom*). Both the Greenland and Tromso profiles indicate that the concentration of BC increases at the snow surface as the snow melts. With only two samples, however, it is too soon to say whether this can be generalized to all arctic soot in snow and, further, the measurements need to be repeated with more attention to the time-evolution of

soot concentration vs. snow loss in order to quantify the fraction of soot which remains at the surface during snow melt.

In the Canadian Arctic, the pre-melt vertical profiles show some indication of higher concentrations at the surface (i.e. in spring; ~5–15 ng/g) than lower down in the snowpack (i.e. in the winter, typically ~2–10 ng/g), but the fraction of absorption due to non-BC constituents is vertically invariant (20–40%). This indicates that the source of the aerosol does not change from winter to spring, but that the magnitude of the source increases or that sublimation is taking place, leaving behind the light-absorbing aerosol. We think the former is more likely since it is consistent with Canadian Arctic springtime boreal forest fires, but neither can be ruled out without detailed snowfall records for the sampled sights. Such records are unfortunately unavailable. The results for the pre-melt Greenland don't show any clear vertical trends, perhaps due to low signal-to-noise at these very low BC concentrations. For the Russian samples, the data fall into three groups: a) higher concentration and higher non-BC fraction at the surface, indicating the addition of biomass burning in spring (Yakutsk and Tiksi); b) lower concentrations and higher non-BC fraction at the surface, indicating both less pollution and a higher relative contribution by biomass burning vs fossil fuel burning in the spring; and c) higher concentrations at the surface but an approximately invariant non-BC fraction, indicating proportionate increases in both fossil and biomass sources and/or consolidation of soot at the surface due to sublimation (Khatanga, Nar'yan Mar and Cherskiy). In fact for much of the arctic snowfall rates are very low and the air is very dry. In many places, such as Cherskiy, there can be long period of dry wind and no new snowfall. Loss of snow via sublimation would certainly lead to higher surface snow soot concentrations, and in some regions this may be a significant driver in determining surface snow soot concentrations. This possibility merits further investigation.

Analysis of these and newly-acquired snow samples is still underway, so the results presented here are preliminary. New samples will be collected through 2010, and we are working on making adjustments for know sources of bias (identified above) as well as improving our technique for separating light absorption due to BC vs. non-BC sources.

References

Bergstrom, R. W., P. Pilewskie, P.B. Russell, J. Redemann, T. C. Bond, P. K. Quinn, and B. Sierau. Spectral absorption properties of atmospheric aerosols, *Atmos. Chem. Phys.*, **7**, 5937–5943, 2007.

Clarke, A. D. and K. J. Noone. Soot in the arctic snowpack: A cause for perturbations in radiative transfer, *Atmos. Env.*, 19(12), 2045–2053, 1985.

Flanner, M.G., C. S. Zender, J. T. Randerson, and P. J. Rasch. Present day climate forcing and response from Black carbon in snow, *J. Geophys. Res.*, 112, D11202, doi:10.1029/2006JD008003, 2007.

Kirchstetter, T. W., T. Novakov and P. V. Hobbs. Evidence that the spectral dependence of light absorption is affected by Organic carbon, *J. Geophys. Res.*, 109, D21208, doi:10.1029/2004JD004999, 2004.

Sun, H., L. Biedermann, and T. C. Bond. Color of brown carbon: A model for ultraviolet and visible light absorption by Organic carbon aerosol, *Geophys. Res. Let.*, 34, L17813, doi:10.1029/2007GL029797, 2007.

Warren, S.G., and W. J. Wiscombe. Dirty snow after nuclear war, *Nature*, 313, 467–470, 1985.

Session 2. Black carbon in Norway

Elemental carbon distribution in Svalbard snow

S. Forsström[1], J. Ström[1,2], C. A. Pedersen[1], E. Isaksson[1] and S. Gerland[1]
[1]Norwegian Polar Institute, Tromsø, Norway; [2]Department of Applied Environmental Science, Stockholm University, Stockholm, Sweden.

The modern climate models include carbonaceous particles in the snow pack. The values used in the models are based on very little or no data as the previous soot measurements in the arctic snow pack are few and mainly from the 1980s. The objective of this work (partly published in Forsström et al 2009) was to study the present-day carbonaceous aerosol particle distribution in snow in Svalbard, and compare these findings to concentrations measured in the air. Further, the atmospheric transport of soot to Svalbard was studied by connecting the atmospheric soot measurements to back-trajectory calculations.
The apparent Elemental carbon (EC, based on a thermal-optical method) content in snow samples collected in Svalbard (European Arctic), during spring 2007 and 2008, was measured. The median EC-concentration of total 181 samples was 4.9 µg l^{-1} (for 2007) and 6.6 µg l^{-1} (for 2008) and the values ranged from 0 to 80.8 µg l^{-1} of melt water. The median concentration is nearly an order of magnitude lower than the previously published data of equivalent Black carbon BC, based on an optical method), obtained from Svalbard snow in the 1980s by Clarke and Noone 1985.

The thermal-optical method divides the carbon on the sample filter to organic, carbonate and apparent Elemental carbon based on different temperatures of volatilization. The optical method, instead, is based on the light absorbance of the matter collected on the filter. To establish a conversion between the results from these two completely different methods is on-going work.

A systematic regional difference was evident, both in 2007 and 2008: EC-concentrations were higher in East-Svalbard compared to West-Svalbard. The observations of snow EC cover spatial scales up to several hundred kilometers, which is comparable to the resolution of many climate models. Figure 1 shows the snow EC concentrations measured 2007. Measurements of atmospheric carbonaceous aerosol (2002–2008) at Zeppelin station in Ny-Ålesund, Svalbard, were divided to air mass sectors based on calculated HYSPLIT (Draxler and Rolph 2003) back-trajectories (Figure 2). The results show that air originating from the eastern sector contains more than two and half times higher levels of soot than air arriving from South-West. This result is in agreement with the findings by Eleftheriadis et al. 2009.

The observed East-West gradient of EC-concentrations in snow may be due to a combination of the atmospheric concentration gradient, the orographic effect of the archipelago, and the efficient scavenging of the carbonaceous particles through precipitation. Regional differences in the amount of precipitation may also influence.

In addition to the gradient in regional scale, a large small scale variability within samples collected at one sampling site (typically within a meter horizontal distance) was discovered. The small scale variability might be connected to post-depositional processes like wind redistribution and evaporation.

References

Clarke A. and Noone K. Soot in the arctic snowpack: A cause for perturbations in radiative transfer, *Atmos. Environ*., 19 (12), 2045–2053, 1985.

Draxler R. and Rolph G. HYSPLIT (HYbrid Single-Particle Lagrangian Integrated Trajectory) Model access via NOAA ARL READY website (http://www.arl.noaa.gov/ready/hysplit4.html). NOAA Air Resources Laboratory, Silver Spring, MD, 2003.

Eleftheriadis K.,Vratolis S. and Nyeki S. Aerosol Black carbon in the European Arctic: Measurements at Zeppelin station, Ny-Ålesund, Svalbard from 1998–2007, *Geophys. Res. Lett.*, 36, L02809, 2009.

Forsström, S., J. Ström, C. A. Pedersen, E. Isaksson, and S. Gerland. Elemental carbon distribution in Svalbard snow, *J. Geophys. Res*, 114, D19112, doi:10.1029/2008JD011480, 2009.

Figure 1. The medians of apparent Elemental carbon (EC) in µg l^{-1} at seven sampling locations in 2007.

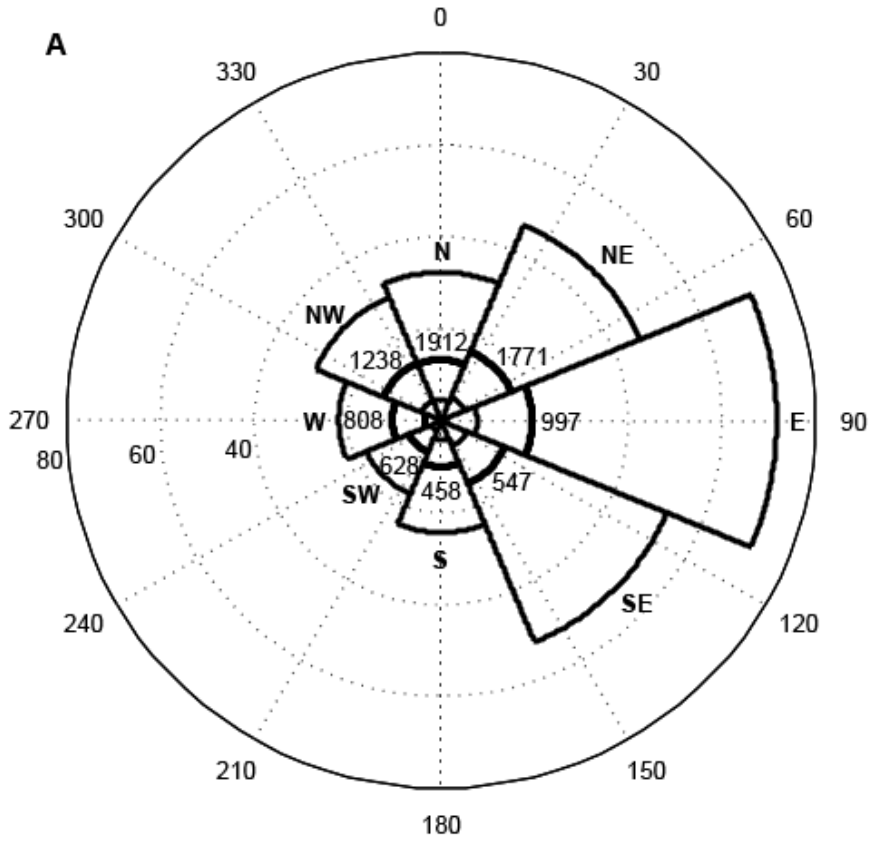

Figure 2. Sector plot showing the connection between the measured air [BC] and the direction of the flow to Zeppelin station according to the back-trajectory runs. The number of trajectories falling into each sector is indicated by the number. The thick arc shows the median of the six-hours mean air [BC] on when the mean vector of the corresponding back-trajectory falls into the sector. The innermost arc indicates the 25 th percentile and the outermost arc the 75 th percentile of the concentration. The axis unit is ngm^3.

Elemental carbon in snow from Norwegian settlements in Svalbard

B. Aamaas[1,2], C. E. Bøggild[2], F. Stordal[1], T. K. Berntsen[1,3], K. Holmén[4], J. Ström[4,5]
[1]Department of Geosciences, University of Oslo, Oslo, Norway,[2]The University Centre in Svalbard, Longyearbyen, Norway; [3]CICERO Center for International Climate and Environmental Research, Oslo, Norway; [4]Norwegian Polar Institute, Tromsø, Norway
[5]Department of Applied Environmental Science, Stockholm University, Stockholm, Sweden.

This material is based on Aamaas' master thesis "Elemental carbon in Svalbard snow from local sources and its impact on surface albedo" defended June 2009. The main objective was to estimate the impact of locally produced Elemental carbon (EC) from Norwegian settlements for entire Svalbard. This was compared to the impact of long-range transported EC found in Svalbard snow. Temporal variability throughout the 2007/08 winter was investigated, as well as the spatial variability in EC concentrations around the settlements.

These objectives were achieved by sampling snow from excavated snow pits along transects. The transects started from the settlements and going radial outwards. These settlements are Longyearbyen (a town of 2000 inhabitants with some local coal mining), Ny-Ålesund (a scientific research station), and Svea (a coal mining town). Snow pits were typically excavated 1–5 km apart. Snow stratigraphy was studied at every snow pit, and a maximum of five snow samples were gathered to represent the different snow layers from the entire annual snow pack. About 1 kg of snow was needed, less if the snow was heavily contaminated. The snow was melted at the lab and, then, filtered through quartz filters as soon as all the snow had melted. The thermo-optical method was used to measure EC on the filters (Birch and Cary, 1996). The NIOSH protocol was followed. EC is observed by a flame ionization detector.

In addition to the local soot sources, there are several coal piles in and around Longyearbyen and Svea. When analyzing the filters, the coal dust is measured as EC. Coal dust fans in the snow can be seen visually from the ground and from raw satellite images. Hence, the coal dust is included in the calculations of the local EC impact.

Extremely high EC concentrations (> 1000 µg/l) were observed around Longyearbyen and Svalbard airport. This extreme spiking is caused by coal dust. The EC concentration drops to about 50 µg/l in Adventdalen and approaches the background level about 50 km to the east. The background EC level for entire Svalbard was determined by Forsström et al. (2009) to be 4.1 µg/l. On Longyearbreen, a glacier about 5 km south of Longyearbyen and at about 500 m a.s.l., the EC concentration was about 17 µg/l during winter. The summer melt caused an increase in the EC concentration, especially in the surface snow layer. The EC concentration in the surface layer in August was a factor 18 of the winter concentration. The increase is caused by melt water draining while the soot particles stay in the snow. Furthermore, wet and dry depositions increase the burden during summer. Spikes in EC concentration were also observed in thick ice lenses. Metamorphosed snow contained more EC than fresh snow in this study.

No clear spiking was seen around Ny-Ålesund. All 50 samples had EC concentrations between 0 and 15 µg/l. The mean concentration was 6.6 µg/l, with a standard deviation which is 65 % of that. Local EC sources cannot be pinpointed in the snow samples even though Ny-

Ålesund certainly is a local source. Elevated EC concentrations are seen in the snow around Svea, and local pollution has clearly a large impact. The mean of the six samples gathered around Svea is 47 µg/l.

A micro scale study was performed 15 km east of Longyearbyen. The snow stratigraphy was examined. Then, snow was gathered from the same snow layers within an area of 5 meters. A large variability was seen in the EC concentration. The mean of all the samples was 57 µg/l, with a standard deviation of 35 %. The standard deviation for the separate sampled snow layers varied between 8 % and 24 %. This variability is mainly caused by natural variability in EC concentrations in the snow pack. Snow is drifting and that results in a mixing of individual snow layers. Hence, the sampling of snow layers from individual precipitation events is difficult.

A relation between EC concentrations and reduced surface snow albedo was calculated from the literature. Soot concentrations were linked to spectral snow albedo by Rypdal et al. (2009) and meshed with incident spectral irradiance given by Grenfell and Perovich (2004). Every snow pit was assumed to represent the surrounding area and halfway to the next snow pit. From this, the impact of local pollution could be determined. The background EC concentration was set to be 4.1 µg/l for entire Svalbard (Forsström et al., 2009). Hence, the albedo reduction from local EC relative to the albedo effect from long-range transported EC for Svalbard was calculated. The best estimate states that Longyearbyen contributes with 2.2 % relative to the long-range transported EC, Svea with 5.4 %, and Ny-Ålesund is set to 0 %. The total is 7.6 %. A high estimate sums up to 9.7 %. There was unusually little sea ice in the Svalbard fjords during the 2007/08 winter. More snow covered sea ice would increase Longyearbyen's impact significantly. In addition, EC from the Russian coal mining town of Barentsburg is not included in these figures. Svalbard covers 61000 km² of land, which is less than 1 ‰ of the entire Arctic. Hence, the local pollution in Svalbard is insignificant for the Arctic as a whole. Long-range transportation contributes with about $2.4*10^2$ t of EC in the annual snow pack in Svalbard, while 5.5 t of EC of local origin was found in the snow pack.

A majority of the snow samples contained dust. A combination of rough topography, available sediments, little vegetation, as well as dry and windy climate favours the transport of Aeolian sediments. A very rough and simple estimate show that dust may be more important at reducing snow albedo than EC in certain areas of Svalbard.

In conclusion, the albedo reduction from EC produced in Norwegian settlements on Svalbard snow is 7.6 % relative to the albedo effect from long-range transported EC. Extremely high EC concentrations are observed locally. There is a large natural variability in EC concentration even on small scales. Melt events will increase the initial EC concentration in the snow pack.

References

Birch, M.E., and Cary, R.A. Elemental carbon-based method for monitoring occupational exposures to particulate diesel exhaust. *Aerosol science and technology*, 25, 221–241, 1996.

Forsström, S., Ström, J., Pedersen, C.A., Isaksson, E., and Gerland, S. Elemental carbon distribution in Svalbard snow. *Journal of Geophysical Research*, 114, D19112, doi:10.1029/2008JD011480, 2009.

Grenfell, T.C. and Perovich, D.K. Seasonal and spatial evolution of albedo in a snow-ice-land-ocean environment. *Journal of Geophysical Research*, 109, C01001, doi:10.1029/2003JC001866, 2004.

Rypdal, K., Rive, N., Berntsen, T., Klimont, Z., Mideksa, T., Myhre, G., and Skeie, R.B. Costs and global impacts of Black carbon abatement strategies. *Tellus*, 61B, 625–641, 2009.

On the temporal and spatial variability of Elemental carbon in snow

J. Ström[1], C. A. Pedersen[1], S. Forsström[1], H. Lihavainen[2], C. Jonasson[3], S. Gerland[1], and E. Isaksson[1]
[1]Norwegian Polar Institute, Tromsø, Norway; [2]Finish Meteorological Institute, Helsinki, Finland; [3]Abisko Research station, Abisko, Sweden

Black carbon content in surface covering the snow season 2007 and 2008 was observed at four different locations in northern Scandinavia and Svalbard. The four different sites used in this study are Tromsø (Norway, 69°39'N, 18°56'E), Abisko (Sweden, 68°21'N, 18°49'E), Pallas (Finland, 67°58'N, 24°07'E), and Austre Brøgger glacier (Svalbard, 67°58'N, 24°07'E). Despite large temporal variations in the concentration of BC in snow, all four sites show an increasing trend over the season. During the snow melting period the increase in BC concentration accelerates. A conceptual view of the seasonal variation of Black carbon concentrations, highlights the importance of considering both the BC content in air as well as the amount of precipitation.

The change in temperature and ice cover within the Arctic is a clear sign of the perturbed global climate (IPCC, 2007). Besides the main climate driver CO_2, studies suggest that even short lived pollutants can potentially have a very significant forcing of the climate. This concerns in particular Black carbon (BC) on snow and ice surfaces. Due to their light absorbing properties these particles transform the incident light energy to heat which enhances the melting of the snow and ice. The possible impact of BC is very large and future increases or decreases in the atmospheric concentrations may have great implications for the arctic climate in the future. However, these estimates of the climate forcing by BC are based on very little basic observations. In this study we present data from one snow season at four different locations.

Measurements of carbon in snow were performed by using the analysis is performed using a Thermal/Optical Carbon Aerosol Analyzer (Sunset Laboratory Inc., Forest Grove, USA). Details of the method can be found in Birch and Cary (1996). The analyzer was operated following the NIOSH method 5040 described in Birch (2003). Speciation between elemental and Organic carbon (EC and OC) is done by the instrument based on the light transmission through the filter substrate. The samples were prepared by collecting snow in plastic bags. The snow was transported to the lab frozen. The snow was placed in a glass jar in a microwave oven and melted on highest effect of 800 W. The time it took to melt the snow depended on the volume, density and snow temperature. However, approximately 10 minutes is a characteristic time. The melted snow was immediately filtered from the glass jar through a quartz microfiber filter (Munktell, 420208, T293). Snow sampling was performed by taking surface snow from approximately the top 5 cm.

Despite large variability on small scales the seasonal development at different sites present several similarities. Figure 1 shows a comparison between Tromsø, Abisko, Pallas and Austre Brøgger glacier near Ny-Ålesund, Svalbard. All four stations show an increasing trend in the snow EC concentration over the season. There are large oscillations related to precipitation and melting events, but an overall increase in EC concentrations with time. The Pallas time series that extend into May clearly shows the rapid increase that suggests that Black carbon particles predominately accumulates at the snow surface and do not significantly follow melt

water through the snow pack. This enhanced increase is also seen in the Brøgger data, but more clear if data is plotted on a linear scale.

As expected, the data from Svalbard shows lower values than the three more southern sites. However, there is no clear difference in the snow concentrations between Tromsø, Abisko, and Pallas. The sampling in Tromsø was conducted in the middle of the town with rather high levels of BC in the air at times. Abisko and Pallas are more remote and therefore expected to be substantially less effected by local sources. The explanation for the similar BC concentration is the difference in the amount of precipitation. Precipitation amount at Abisko and Pallas is around 300 mm and 500 mm yr^{-1}, respectively. In Tromsø the precipitation was 356 mm during the studied 5 months only.

We can conceptually understand the seasonal variation by making some very simplified assumption and using constant values of dry deposition velocity and wet scavenging ratio. Four different sites are characterized by the length of the snow season, a constant BC concentration in the air, amount of precipitation during the snow season, and loss of water during the snow season. The last parameter can be viewed as sublimation and is taken as a constant rate over the snow season. The first place is a wet and polluted site, which is named "Tromsø". The second site is less polluted, but also a dryer site. It is named "Abisko". The third and forth site are clean with the same BC concentration in the air but differ in the amount of precipitation. These sites are named "Wet Svalbard" and "Dry Svalbard". The naming is done to easier relate to the observations, which is why the names are in quotes. The values used are listed in Table 1.

By multiplying the dry deposition velocity with the BC concentration and time, we arrive at the amount of BC that is deposited per square meter over the snow season. Analogous, we can calculate the amount that is scavenged by precipitation. The sum is the total amount of BC deposited in the snow during the season. The numerical values for the four hypothetical sites are listed in Table 2.

If all the BC is distributed over the total amount of precipitation, one would reach a concentration that perhaps reflect the mean early season before there has been any great loss of water from the surface snow. Later in the season there would be less of the total precipitation remaining and this will cause the concentration of BC to increase. If we divide all the BC with the last remaining 10 mm of precipitation we can view this as the end of the season. The resulting concentrations are listed in Table 2, and illustrated in Figure 2.

Although the data in Figure 2 is based on highly idealized conditions, the results provide a conceptual view of why two different sites like Tromsø (dirty and wet) and Abisko (clean and dry) can present comparable BC concentrations in the snow. Towards the end of the season we expect the difference to be larger because it is the total deposited amount of BC that will be important then.

Our two examples (Wet- and Dry-Svalbard) illustrate the effect of different precipitation amounts, but with same BC content in the air. There are large regional differences on Svalbard, with respect to precipitation. Ny-Ålesund for example has about 400 mm yr^{-1}, whereas Svea ca. 160 km to the South-East only have 200 mm yr^{-1}. Towards the end of the season, the BC concentrations in the snow would become more similar at the wet and the dry site. As stated above, it is the total accumulated BC that counts when the snow melts away.

Hence, to mitigate the effect of BC in arctic snow, it is not enough to focus on the spring season. The whole season must be considered.

References

Birch, M. E. Elemental carbon (diesel exhaust): Method 5040, in *NIOSH Manual of Analytical Methods*, National Institute of Occupational Safety and Health, Cincinnati, Ohio, 2003.

Birch, M. E., and R. A. Cary. Elemental carbon-based method for monitoring occupational exposures, to particulate diesel exhaust, *Aerosol. Sci. Technol*., 25, 221– 241, 1996.

Intergovernmental Panel on Climate Change. *Climate Change 2007 - The Physical Science Basis: Contribution of Working Group I to the Fourth Assessment Report of the IPCC*. Cambridge: Cambridge University Press. ISBN 978 0521 88009-1, 2007.

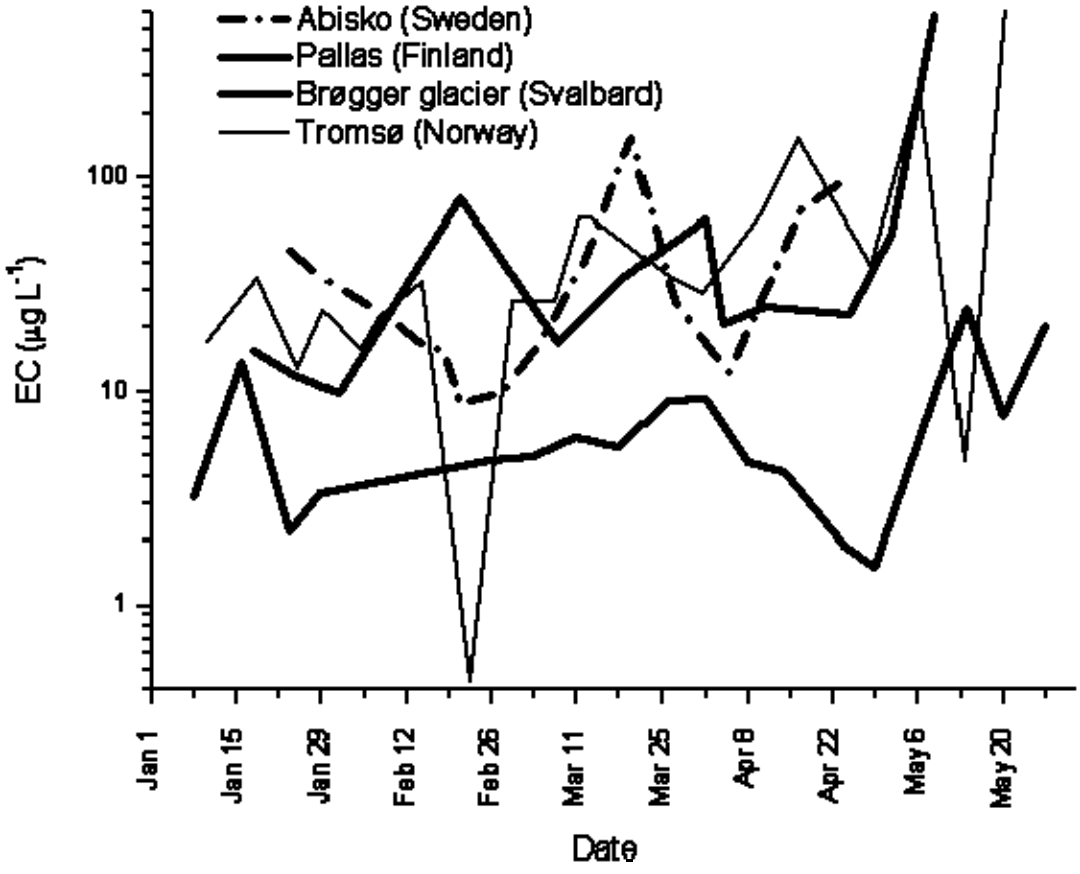

Figure 1. Seasonal evolution of BC (or EC, Elemental carbon) in surface snow (top 5 cm) at four different locations.

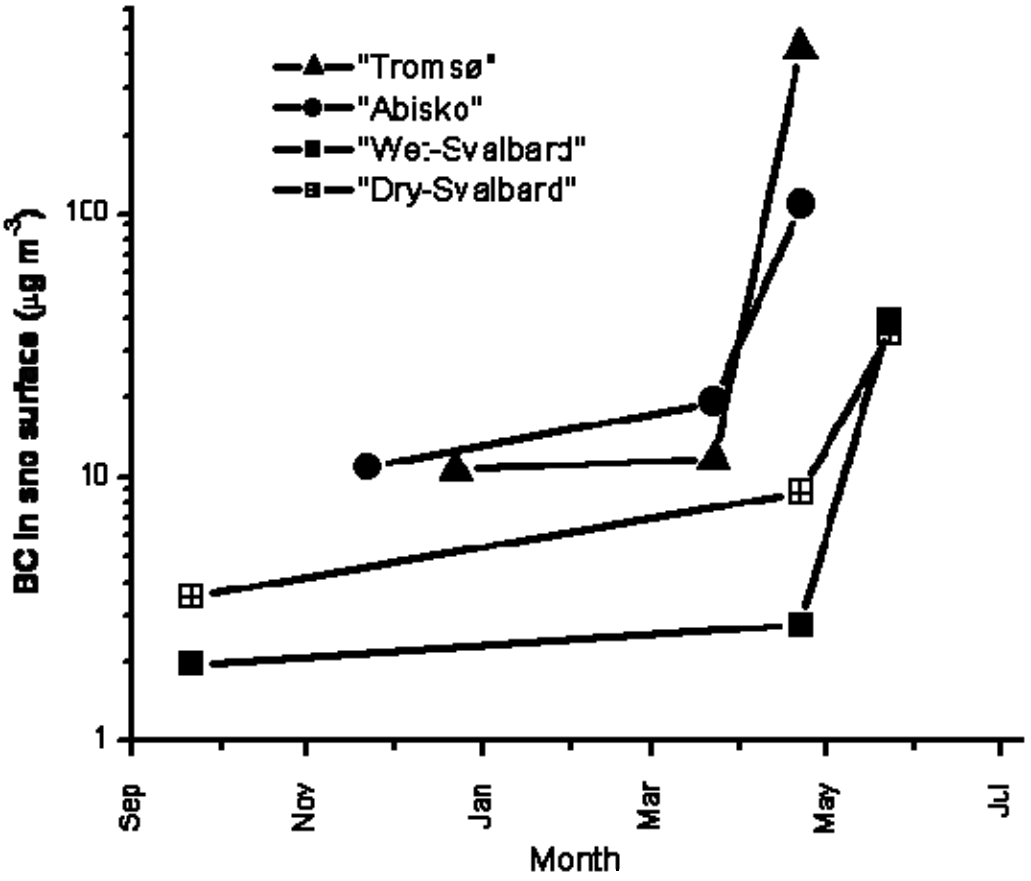

Figure 2. Graphical presentation of the numerical results presented in Table 2.

Site	Snow cover	Winter/Spring BC concentrations (μg m^{-3})	Winter/Spring precipitation (mm)	Water lost from snow cover (mm)
"Tromsø"	Jan/May	0.6	400	40
"Abisko"	Dec/May	0.2	100	45
"Wet Svalbard"	Oct/Jun	0.05	200	60
"Dry Svalbard"	Oct/Jun	0.05	100	60

Table 1. Parameters characterizing four hypothetical sites given association names in column one.

Site	Dry Dep. (g m^{-2})	Wet Dep. (g m^{-2})	Total Dep. (g m^{-2})	Early Season (μg L^{-1})	Late season (μg L^{-1})	End season (μg L^{-1})
"Tromsø"	2.33	1.92	4.25	10.6	11.8	425
"Abisko"	0.93	0.16	1.09	10.9	19.9	109
"Wet Svalbard"	0.31	0.08	0.39	1.9	2.8	39
"Dry Svalbard"	0.31	0.04	0.35	3.5	8.8	35

Table 2. Calculated values based on values in Table 1 and a dry deposition velocity of 0.03 cm s^{-1} and a precipitation scavenging ratio of 8. Early season is total deposited Black carbon divided by all precipitation. Late season is total deposited Black carbon divided by precipitation minus water lost. End season is total deposited Black carbon divided by 10 mm precipitation.

Session 3. Effects of Black carbon on albedo and remote sensing

The effect of Black carbon particles on snow albedo derived from *in-situ* measurements

C. A. Pedersen[1], J. Ström[1], S. Forsström[1], S. Gerland[1], and S. R. Hudson[1]
[1]Norwegian Polar Institute, Tromsø, Norway

Snow covered surfaces have a high albedo and most of the incoming solar radiation is reflected. The natural snow albedo variability is large, and the wavelength dependent snow albedo is affected both by snow physical parameters (snow grain size and snow depth) as well as variability in the atmospheric conditions (solar zenith angle and cloud cover; Wiscombe and Warren, 1980). Black carbon (BC) particles emitted from incomplete combustion of fossil fuel and biomass, are transported to the Arctic where they deposit on the snow, darken the surface, and reduce the albedo. The direct snow albedo effect of BC has previously been modeled (Jacobsen, 2004; Warren and Wiscombe, 1980), however, very few in-situ field measurements exists that support the modeling results. The one exception is Grenfell et al. (1981), but that study only included two sets of corresponding measurements of spectral albedo and BC in snow. What has been done in the past is that levels of BC in the snow have been measured or estimated, and models have been used for inferring the albedo effect.

Here we present an extensive set of corresponding *in situ* measurements of spectral snow albedo, BC levels in the snow, as well as snow physical parameters and atmospheric conditions. From this dataset we are able to separate the BC signature on the optical properties of snow from the natural snow albedo variability, and we thereby provide the missing component of an extensive set of data to compare previous modeling results with. This extended abstract is a preliminary summary of results that will be published elsewhere later.

The *in situ* measurements are from various field campaigns over the years 2006, 2007 and 2008, covering sites at Svalbard, mainland Norway, Northern Alaska, and sea ice in the Fram Strait, including in total 40 concurrent measurements of optics, BC levels, and snow properties. The details of the measurement approach are as follows: For each snow sample, about 1–2 l of snow from the upper 5-cm of the snow pack was collected. Most snow samples were kept frozen until the time for analysis when they were fast melted in a microwave oven. However, a few snow samples were melted in the glass jars, and stored melted for longer times. The melted water (typically about 0.5–1.0 l) was filtered through quartz substrates using a small vacuum pump. The filters were analyzed with a thermo-optical method, using the Thermal/Optical Carbon Aerosol Analyzer (Sunset Laboratory Inc., Forest Grove, USA), and NIOSH 5040 protocol (Birch and Cary, 1996). The carbon on the filter was divided between organic (OC) and elemental (EC) carbon based on the optical procedure that compensate for pyrolysis or charring of OC. The resulting EC is used as a proxy for the BC aerosol.

The optical properties of the snow surfaces (spectral albedo and spectral reflectance factor) were measured with two different spectroradiometers; Fieldspec Pro (Analysis Spectral Device, Boulder, USA) and Ramses VIS (TriOS, Oldenburg, Germany), covering wavelength ranges of 350–2500 nm and 320–950 nm, respectively. The optical data have been corrected for shadows to include: shadow on the surface from the sensors and albedo pole (affecting F↑), and tripod/vertical pole blocking a portion of F↑. These corrections are in the order of

1.0%, and are extremely important as a 1.0% reduction in spectral albedo for new snow at 470 nm imply BC to increase from 0 to 13 ng/g in the radiative transfer model of Warren and Wiscombe (1985). Albedos above 1.0, due to sloping surfaces, and cases of clear sky where the solar zenith angle was above 85º were removed from the dataset. The snow physical properties of the uppermost snow layer (snow grain size and snow type), snow depth, temperature and light conditions were also collected.

The lowest concentrations of EC were found in Ny-Ålesund (Svalbard) and Barrow (Northern Alaska) and were in the range 5–11 ng/g and 3–14 ng/g, respectively. At the same time, those were the sites with the highest spectral albedo (range 0.89–0.99 and 0.96–0.97, respectively) and (for the most) the smallest snow grain sizes. The highest Elemental carbon concentrations were found in urban Tromsø area (range from 0 ng/g after a new snowfall to 878 ng/g for the last snow in spring), corresponding in time with relative lower spectral albedo and larger snow grain sizes.

The linear correlation coefficient (ρ) between snow albedo and EC concentration in snow is negative for all wavelengths, relating an increasing amount of BC to a decreasing albedo. ρ is highest at the shortest wavelengths (0.77 at 350 nm), because the ice absorption is at its minimum here (Warren and Brandt, 2008), which leads to highest sensitivities to BC. ρ slightly decreases (in absolute value) with wavelength, however, it stays high into the near infrared (NIR) range. Previous results indicate that BC has a negligible effect at longer wavelengths (above 900 nm) as the ice absorption itself is so large (Warren and Wiscombe, 1980). At the longer wavelengths the snow grain size is the dominating factor (Wiscombe and Warren, 1980), which then implies a strong relationship between BC and snow grain size in our measurements. This intuitively seems right as bulk of the BC transport occurs in the spring together with less new snow fall (metamorphosed snow with larger grains), and also since BC particles in the snow enhance grain growth. In addition there are indications that BC tends to accumulate on the surface for melting snow (Ström, this report). The measurements indeed show this co variety, although the linear correlation coefficient between BC and snow grain size is relative weak. The semi-discrete values for the grain sizes (visually determined by an observer with mm-sheet and a loupe, and biased by the observers tendency to approximate the observations to the closest round value) is probably the explanation.

The albedo BC effect is parameterized based on fitting the measurements to the model $y = A - B \cdot x^C$, where y is the spectral albedo, x is the EC level, and the parameters A, B, and C are found from the least-mean-square fit of the measurements to the model for each wavelength. A, B, and C were found to vary smoothly with wavelength (λ), and were fitted to a second order polynomial: $a \cdot \lambda^2 + b \cdot \lambda + c$. This parameterization was developed without any sorting on snow grain size.

The parameterization indicates that the albedo reduction compared to clean snow at 470 nm is 0.4%, 1.5% and 5.4%, for BC content in the snow of 1 ng/g, 10ng/g and 100 ng/g, respectively. This compares well with the corresponding ranges (range between new snow and old melting snow) from Warren and Wiscombe model (1985) at 0.1–0.4%, 0.8–2.7% and 4.2–11.8%. There is no clear tendency that the parameterization for smaller BC levels is more similar to model results for new snow (smaller grains), and vica versa. We are currently working on comparing the measurements against an updates Warren and Wiscombe (1980) model.

To conclude, this study is purely empirical, and its limitation is the data quality and the number of measurements. The data quality is mainly restricted by the accuracy of the spectral albedo measurements, particularly since the data was collected using two different sensors, and a few of the measurements were reflectance factor, not albedo. Also, the parameterization was forced by few measurements of high EC levels.
However this is not affecting the main results of this study, which is, for the first time to confirm the effect BC particles in snow has on reducing the spectral snow albedo through an ample set of *in-situ* measurements. It is also important to note that we were able to detect a BC signal, even for low levels of BC in the snow and it emphasize the climate sensitivity even for low BC levels.

References

Birch, M. E., and R. A. Cary. Elemental carbon-based method for monitoring occupational exposures, to particulate diesel exhaust, *Aerosol. Sci. Technol*., 25, 221– 241, 1996.

Clarke, A.D. and Noone, K.J. Soot in the arctic snowpack: A cause for perturbations in radiative transfer. *Atmos. Environ.*, 19(12), 2045–2053, 1985.

Grenfell, T. C., D. K. Perovich and J. A. Ogren. Spectral albedos of an alpine snow pack, *Cold Reg. Sci. Technol., 4*, 121–127, 1981.

Jacobson, M. Z. Climate response of fossil fuel and biofuel soot, accounting for soot's feedback to snow and sea ice albedo and emissivity. *J. Geophys. Res.*, 109(D21201), 2004.

Warren, S.G., and R.E. Brandt. Optical constants of ice from the ultraviolet to the microwave: A revised compilation. *J. Geophys. Res*., 113, D14220, doi:10.1029/2007JD009744, 2008.

Warren, S.G. and Wiscombe, W.J. A model for the spectral albedo of snow. II: Snow containing atmospheric aerosols. *J. Atmos. Sci*., 37, 2734–2745, 1981.

Warren, S.G. and Wiscombe, W.J. Dirty snow after nuclear war. *Nature*, 313, 467–470, 1985.

Wiscombe, S. and Warren, S.G. A model for the spectral albedo of snow. I: Pure Snow. *J A S*, 37:2712–2733, 1980.

Relating Black carbon content to albedo reduction

R. E. Brandt[1] and S. G. Warren[1]
[1]Deptartment of Atmospheric Science, University of Washington, Seattle, Washington, USA

The dependence of snow albedo on impurity content was first quantified by radiative transfer modeling (Warren and Wiscombe, 1980), which computed large reductions of albedo at visible wavelengths for parts-per-million (ppm) amounts of soot. However, in remote snow of the Northern Hemisphere, the levels of soot pollution are in the parts-per-billion (ppb) range, not ppm (Clarke and Noone, 1985), where the effect on albedo is at the level of a few percent. A reduction of albedo by 1–2% is significant for climate but is difficult to detect experimentally, because snow albedo depends on several other variables. In our work to quantify the climatic effect of Black carbon (BC) in snow, we therefore do not directly measure the albedo reduction. Instead, we use a two-step procedure: (1) We collect snow samples, melt and filter them, and analyze the filters spectrophotometrically for BC concentration (Grenfell et al., this report). (2) We use the BC amount from the filter measurement, together with snow grain size, in a radiative transfer model to compute the albedo reduction.

The quantity required for radiative transfer modeling is the absorption coefficient k_{abs}, in units of m^2/(g snow). From the filter measurement, this is obtained as the absorption cross-section of particles on the filter, divided by the mass of meltwater passed through the filter. For convenience in relating our results to the predictions of atmospheric transport and deposition models, we convert k_{abs} to a concentration C of BC in snow:

$$k_{abs}=B_aC,$$

where C has units (g BC) / (g snow), and B_a is the mass-absorption cross-section (MAC) of BC (m^2/g). Our filters are calibrated relative to filters containing weighed amounts of Monarch-71 soot, whose MAC was determined by optical analysis of the spectrophotometer to be $B_a \approx 6$ m^2/g (A. Clarke, personal communication).

The computed reduction of snow albedo is model-based, so it requires experimental verification. We doubt that direct measurement of albedo-reduction will be feasible in nature, because of the vertical variation of both snow grain size and soot content, and because the natural soot content is small. Furthermore, deep snow would be required, because the spectral signature of sooty snow is the same as that of thin snow (reduction of visible albedo but not near-infrared albedo; compare Figure 13 of Wiscombe and Warren (1980) to Figure 7 of Warren and Wiscombe (1980)). Also, accurate knowledge of the instrument's shadowing correction would be needed, because its value is typically ~1%; i.e., of similar magnitude to the albedo reduction for typical soot amounts in Northern Hemisphere snow. For example, in the experiment described below, the shadowing correction was estimated as 1.7%, but is uncertain to perhaps a factor of 2. The inferred values of B_a for soot, with and without applying a shadowing correction, differ by only 10%, whereas in natural snow with only ~6 ppb soot the inferred B_a values could differ by a factor of 10 or more.

We conclude that what is needed is an artificial snowpack, with uniform grain size and large uniform soot content (ppm not ppb), to produce a large signal on albedo. The experiment can be done in a freezer-laboratory or outdoors. The experiment we are pursuing is done outdoors. The reasons for choosing this approach are as follows:

(1) The snowpack in the field of view is uniformly illuminated if the source of radiation is the Sun.
(2) Visible radiation penetrates tens of centimeters into snow, so photons emerge horizontally distant from where they entered. In the limited width of a laboratory snowpack, radiation may be absorbed by the walls of the container.
(3) In a laboratory experiment only a narrow field of view can be measured, rather than a hemispheric field of view, so a laboratory experiment measures the bidirectional reflectance for particular angles rather than albedo.

The disadvantage of an outdoor experiment is that one must wait for appropriate weather: low temperature (-20 to -40°C), calm winds, diffuse incidence, and no snow falling during the experiment.

The experiments were carried out on an open field behind the school at Bloomingdale, New York. A small snowmaking machine, using the village water supply, could make a snowpack of area 75 m^2 and depth 15 cm in a period of 4 hours, deposited over a 40-cm natural snowpack. A soot suspension was maintained in a soniccated bath, which could be entrained into the water stream. The snowmaking operation typically began about midnight. Two snowpacks were made side-by-side, with and without added soot. For a soot content of 1 ppm, 3 g soot were dispersed into 3 tons of snow. The Bloomingdale water supply was quite clean, with soot content <6 ppb, considerably cleaner than newly fallen snow, which contained soot from residential wood-burning stoves in the surrounding region.

The artificial snow grains were quasi-spherical. They were ejected from the nozzle as droplets, which froze in the cold air, so the soot particles were probably uniformly distributed within each droplet.

The most successful of the experiments so far was the trial of 5 February 2009, which used Aquablack 162, a hydrophilic soot. The spectral albedos of the two snowpacks were in agreement for near-infrared wavelengths $\lambda > 1.0$ μm, but diverged at shorter wavelengths, as expected. The shadowing correction for diffuse incidence was estimated by geometric analysis as 1.7%. The observed albedos were therefore multiplied by 1.017 before further analysis.

The sooty snowpack was modeled as an external mixture of soot spheres and ice spheres. The soot size distribution was modeled as lognormal, with mode radius 65 nm and lognormal width 1.3. This size distribution was chosen to resemble an ambient size distribution, but it also closely mimics the Aquablack size distribution. Its mass-absorption cross-section at λ = 550 nm is B_a = 6.9 m^2/g. The BC content of the model was adjusted until the model matched the observed albedo reduction as a function of wavelength; this required C=2.25 ppm.

After completing the albedo measurements, samples of the two snowpacks were collected, melted, and filtered through 0.4-μm nuclepore filters. The filter transmittances, compared to the reference filters assuming B_a = 6 m^2/g, implied 6 ppb for the clean water and 1.3 ppm for the sooty snowpack.

The BC amount inferred from the albedo measurements, relative to that inferred from the filter transmission, is (2.25 ppm × 6.9 m^2/g) / (1.3 ppm × 6 m^2/g) = 2.0. This result suggests that BC inside a snow grain is twice as efficient as BC on a filter, and that BC inside the snow has $B_a \approx$ 12 m^2/g. A possible explanation is that soot in artificial snow is probably

located in the interior of the frozen drops, so its MAC is enhanced relative to an external mixture (Ackerman and Toon, 1981). In natural crystals of falling snow, soot can be collected by both nucleation and below-cloud scavenging, so in the snowpack the soot particles may be on the surface of snow grains as well as in the interior, and the MAC will therefore most likely be intermediate between 6 and 12 m^2/g.

Further experiments are planned for the winter of 2009–2010.

Acknowledgments
The principal of Bloomingdale Elementary School, Pat Hogan, kindly made available the necessary utilities and space for the snowmaking experiment. Sarah Doherty, Kristel Guimara, Christina Pedersen, and Ellen Beberman assisted with the experiments. The research was supported by NSF grant ARC-06-12636.

References

Ackerman, T.P., and O.B. Toon. Absorption of visible radiation in atmosphere containing mixtures of absorbing and nonabsorbing particles. *Appl. Opt.*, **20**, 3661–3668, 1981.

Clarke, A.D., and K.J. Noone. Soot in the arctic snowpack: A cause for perturbations in radiative transfer. *Atmos. Environ.*, **19**, 2045–2053, 1985.

Warren, S.G., and W.J. Wiscombe. A model for the spectral albedo of snow, II: Snow containing atmospheric aerosols. *J. Atmos. Sci.*, **37**, 2734–2745, 1980.

Wiscombe, W.J., and S.G. Warren. A model for the spectral albedo of snow, I: Pure snow. *J. Atmos. Sci.*, **37**, 2712–2733, 1980.

Darkening of soot-doped natural snow: Measurements and model

C. S. Zender[1,2], F. Dominé[1], J.-C. Gallet[1], G. Picard[1]
[1]Laboratoire de Glaciologie et Géophysique de l'Environnement, Grenoble, France
[2]Department of Earth System Science University of California, Irvine, California, USA

We conducted the first measurements of the direct effect of laboratory controlled BC-contamination on snow albedo in a laboratory environment. Optical measurements of natural snow intentionally doped with industrial grade BC were conducted at visible and near-infrared wavelengths. Snow albedo was measured in a (portable) integrating sphere system. The absolute spectral albedos are less than expected at visible wavelengths due to absorption by the sample holder which is too shallow to present a semi-infinite sample surface. Hence we focus on the albedo change by BC doping, rather than on the absolute snow albedo itself. Using preliminary calibrations, our measurements agree well with model predictions that BC concentrations from 1–200 ppmm reduce albedo by 5–70%. A key uncertainty is assessing how much BC mass was "lost" during the doping process and thus did not fully contribute to snow darkening.

Light-absorbing impurities including Black carbon (BC) and dust reduce snow and ice reflectivity (Warren and Wiscombe, 1980; Chýlek et al., 1983) and can thereby trigger ice-albedo feedbacks (Warren, 1984, e.g.,). If our representation of the associated processes in climate models is adequate, then snow-darkening by anthropogenic BC deposition is a major contributor to recent arctic warming (Hansen and Nazarenko, 2004; Jacobson, 2004; Flanner et al., 2007; Quinn et al., 2008). Here we report the first laboratory measurements of the direct effect of laboratory controlled BC-contamination on natural snow albedo.
BC darkens snow and alters climate through a series of processes that climate models approximate with varying degrees of uncertainty. The fundamental cause of snow darkening is the contrast between the single scattering albedo of BC, the darkest aerosol, and that of snow, the brightest surface. These single scatter albedos depend, respectively, on the chemical composition, structure, and mixing state of BC (Bond and Bergstrom, 2005), and on the size and shape of snow crystals (Warren and Wiscombe, 1980; Grenfell and Warren, 1999). Models show that 15 ppbm (parts-per-billion-by-mass) of BC externally mixed in snow of optically-equivalent effective radius r_e = 100μm will darken the snow albedo by about 1% at the mid-visible wavelength λ = 500 nm (Grenfell et al., 1994).

Previous measurements of the albedo perturbation of snow by BC have, to our knowledge, tested snow with *a* priori unknown (rather than known) amounts of BC. Typically field snow samples are first collected, melted and filtered. Filters may then be analyzed using thermo-optical techniques to measure Elemental carbon, organic, and/or total carbon mass concentration (Legrand et al., 2007). A separate approach that requires only optical techniques compares the filter transmission to the transmission observed from known amounts of a "standard" type of commercially available BC (Noone and Clarke, 1988; Warren and Clarke, 1990). From this one estimates the mass concentration of the standard BC which would have caused the same filter transmission. This method has the advantage of expressing the BC mass in terms of the mass of a well-studied type of BC, facilitating intercomparisons. This optically equivalent BC mass concentration may then be used to estimate the (and/or compare to the field-measured) snow albedo.

Our experiments attempt to perturb the snow albedo with an *a priori* known mass of BC, and then to measure its albedo perturbation. The intent is to test the adequacy and fidelity of forward radiative transfer model treatments of BC under varying conditions, eventually to include other contaminants (e.g., dust) and coatings. To accomplish this we dope natural snow with pre-measured quantities of BC and observe the resulting albedo perturbation.

Our procedure measure the perturbation to snow albedo by BC follows these steps. 1. Collect fresh surface snow. 2. Weigh BC 3. Weigh snow 4. Separately blend control and BC-doped snow samples 5. Dilute snow samples as necessary 6. Measure snow density 7. Measure 1310 nm-reflectance 8. Measure 630 nm-reflectance

We collected surface snow for these experiments during short expeditions to nearby Chamrousse Ski Station (elevation ~ 1750 m). To minimize accumulation of impurities, all specimen collection took place within 24-hours of snowfalls lasting at least 24-hours. Any impurities present in the fresh snow samples contribute to excess absorption in both the clean and doped snow experiments described below.

Prior to collection we measured *in situ* properties (air and snow temperature, snow density and stratigraphy). Near surface air temperature never exceeded T = −0.5º C between snowfall and collection. Surface specimens (top ~ 50 cm) were transported to LGGE. All subsequent handling, preparation, and measurement of snow took place in a constant-temperature (−15º C) cold-room facility at LGGE.

We doped snow with commercially available Monarch 120 Carbon Black supplied by Cabot Corporation (Billerica, MA, USA). Monarch 120 is most similar to the discontinued product Monarch 71 used to calibrate optically effective BC concentration in many previous studies (e.g., Clarke and Noone, 1985; Warren and Clarke, 1990; Clarke et al., 2004) (S. Warren, personal communication, 2007). Monarch 120 is not, strictly speaking, soot (Watson and Valberg, 2001), nor is it pure Elemental carbon (EC). Monarch 120 is our experimental analogue for light-absorbing carbon (Bond and Bergstrom, 2005) aerosol in the climate system, and we refer to it simply as BC henceforth.

BC samples of 3–100 mg were weighed on a precision scale, then mixed into the snow specimens of approximately 440 g. Mixing was accomplished with a commercially available blender composed of aluminum and stainless steel. Blending for one minute, adding BC, then blending for 2.5 minutes produced darkened snow that appeared homogeneous. This mixing procedure created doped snow with initial BC mixing ratios 7.5 q_{BC} 221 ppmm. Some of this material was diluted with clean snow in the blender to obtain BC mixing ratios as low as q_{BC} = 250 ppbm. One minute of additional blending was performed per dilution stage.

Blank snow specimens were created with the same procedure, but without adding BC. To prevent contamination, separate sets of mixing elements were maintained for the blanks and doped samples. All components were washed in 18 MΩ-cm water between uses, and no residual BC was noticed on the mixing elements.

The key optical measurements were made with DUFISSS, the DUal-Frequency Integrating Sphere for Snow SSA measurement, which is more fully described in Gallet et al. (2009), hereafter GDZ09. Collimated radiation from diode lasers strikes a snow sample flush with the sphere bottom. After multiple scattering, the diffuse radiation striking an InGaAs photodiode is converted to a voltage. The photodiode sits behind an optical baffle to screen-out specular

reflection. The voltage-to-reflectance conversion is calibrated by measurements of reflectance standards (Sphere Optics Inc.) made before and after snow sample measurement. Our experiments used two diode-lasers (635 and 1310 nm) to measure the visible and NIR snow albedos, A_{635} and A_{1310}, respectively.

Snow reflectance is primarily determined by it specific surface area (SSA), the surface-area-to-mass ratio (Grenfell and Warren, 1999). SSA is inversely related to the optically effective snow grain size, aka effective radius r_e. Snow NIR reflectance is highly correlated with SSA (Domine et al., 2006), and is insensitive to small amounts of impurities. GDZ09 describe how we calibrate 1310 nm reflectance A_{1310} to SSA measured by methane adsorption techniques.

Snow albedo simulations were performed with the Shortwave Narrow Band (SWNB2) radiative transfer model (Zender ,1999; Zender and Talamantes, 2006). SWNB2 solves for all radiant quantities at 10 cm^{-1} spectral resolution from 0.2–5.0 μm using the discrete ordinates technique. Ice refractive indices at 635 and 1310 nm values are as in Warren and Brandt (2008). Snow samples were treated as plane-parallel and homogeneous (constant density with depth). Edge effects are discussed below.

Model inputs include the snow density (measured), snow SSA (estimated from 1310 nm reflectance as in GDZ09), and the geometric standard deviation σ_g of the snow grain size distribution. Grenfell and Warren (1999) found σ_g =1.6 is typical at the South Pole, and Flanner and Zender (2006) showed σ_g =2.3 best fits observed grain-size evolution for young snow, and Gallet et al. (2009) found σ_g =1.4 best matches reflectance measurements at λ = 1550 nm. The modeled reflectance for σ_g =2.3 is greater than that for σ_g =1.4 by about 0.8% and 1.1% for λ = 635 and 1310 nm, respectively. This study uses σ_g =2.3 for consistency with the SNICAR model.

Our treatment of BC optical properties is identical to Flanner et al. (2007). Spectral variation of the BC refractive index is from Chang and Charalampopoulos (1990). A lognormal BC size distribution is assumed with number-median radius 50 nm and geometric standard deviation σ_g =1.5. Tuning the BC density to 1322 kg m^{-3} leads to a mass absorption coefficient ψ = 7500 m2 kg^{-1} at λ = 550 nm, in agreement with the central estimate of Bond and Bergstrom (2005). We perform sensitivity studies to the effects of sulfate coatings on BC. These coatings increase the mass absorption coefficient relative to uncoated BC of the same mass by a factor of about 1.6 (Bond et al., 2006).

We report here reflectance measurements from N = 97 individual snow samples. Samples were either clean (not doped) or doped with one of six BC mixing ratios q_{BC} between 250 ppbm and 221 ppmm. Gallet et al. (2009) describe calibration of the NIR albedo with DUFISSS. These calibration parameters have not yet been confirmed for visible albedos. Pending the completion of this, we have employed a simpler, preliminary calibration that results in the modeled data shown in Figures 1a and b. The preliminary calibration simply assumes, based on least squares fits, that the conversion between plane-parallel semi-infinite albedos and DUFISSS measurements (which are neither plane-parallel nor semi-infinite) and is accomplished by multiplying the model estimates by 0.91 and 0.77 for visible and NIR albedos, respectively. This method yields an RMS bias of 0.75% (absolute) to 1.3% (relative) between modeled and measured albedo. A key uncertainty, not yet tackle, is verifying how much BC mass was “lost” during the doping process and thus did not fully contribute to snow darkening.

A series of further simulations (not shown) was conducted to assess the effect of different model assumptions on the model-measurement disparity. We found that using specific surface area (inferred from 1310 nm reflectance) improves visible snow albedo predictions (at 635 nm). The model-measurement disparity also improved when we assumed externally mixed uncoated BC rather than externally mixed sulfate-coated BC.

We measured the change in visible snow albedo due to doping the snow with six differing amounts of BC. Using a preliminary calibration, the albedo was within ~ 1% of predictions throughout the measured range of BC concentration, from 250 ppbm to 221 ppmm. These results must be considered preliminary pending completion of the visible albedo calibration, and verification of the BC mass which affected snow albedo.

Acknowledgments
Supported by NSF ARC-0714088, NASA NNX07AR23G, and CNRS. We thank M. G. Flanner, T. Grenfell, J.-L. Jaffrezo, T. Kirchstetter, and S. Warren. Download this manuscript from http://dust.ess.uci.edu/ppr/ppr ZGD09.pdf.

References

Bond, T. C., and R. W. Bergstrom. Light absorption by carbonaceous particles: An investigative review, *Aerosol Sci. Technol.*, *40*(1), 27–67, doi:10.1080/02786820500421,521, 2005.

Bond, T. C., G. Habib, and R. W. Bergstrom. Limitations in the enhancement of visible light absorption due to mixing state, *Submitted to J. Geophys. Res.*, *111*(D20), D20, 211, doi:10.1029/2006JD007,315, 2006.

Chang, H., and T. T. Charalampopoulos. Determination of the wavelength dependence of refractive indices of flame soot, *Proc. Roy. Soc. London A, Math. and Phys. Sci.*, *430*(1880), 577–591, 1990.

Chýlek, P., V. Ramaswamy, and V. Srivastava. Albedo of soot-contaminated snow, *J. Geophys. Res.*, 88, 10,837–10,843, 1983.

Clarke, A. D., and K. J. Noone. Soot in the arctic snowpack: A cause for perturbations in radiative transfer, *Atmos. Env.*, *19*(12), 2045–2053, 1985.

Clarke, A. D., et al. Size distributions and mixtures of dust and Black carbon aerosol in Asian outflow: Physiochemistry and optical properties, *J. Geophys. Res.*, *109*(D15S09), doi:10.1029/2003JD004,378, 2004.

Domine, F., R. Salvatori, L. Legagneux, R. Salzano, M. Fily, and R. Casacchia. Correlation between the specific surface area and the short wave infrared (SWIR) reflectance of snow, *Cold Reg. Sci. Tech.*, *46*, 60–68, doi:10.1016/j.coldregions.2006.06.002, 2006.

Flanner, M. G., and C. S. Zender. Linking snowpack microphysics and albedo evolution, *J. Geophys. Res.*, *111*(D12), D12,208, doi:10.1029/2004GL022,076, 2006.

Flanner, M. G., C. S. Zender, J. T. Randerson, and P. J. Rasch. Present-day climate forcing and response from Black carbon in snow, *J. Geophys. Res.*, *112*, D11, 202, doi:10.1029/2006JD008,003, 2007.

Gallet, J.-C., F. Dominé, C. S. Zender, and G. Picard. Measurement of the specific surface area of snow using infrared reflectance in an integrating sphere at 1310 and 1550 nm, *The Cryosphere*, *3*(2), 167–182, 2009.

Grenfell, T. C., and S. G. Warren. Representation of a nonspherical ice particle by a collection of independent spheres for scattering and absorption of radiation, *J. Geophys. Res.*, *104*(D24), 31,697–31,709, 1999.

Grenfell, T. C., S. G. Warren, and P. C. Mullen. Reflection of solar radiation by the Antarctic snow surface at ultraviolet, visible, and near-infrared wavelengths, *J. Geophys. Res.*, *99*(D9), 16,669–18,684, 1994.

Hansen, J., and L. Nazarenko. Soot climate forcing via snow and ice albedos, *Proc. Natl. Acad. Sci.*, *101*(2), 423–428, 2004.

Jacobson, M. Z. The climate response of fossil-fuel and biofuel soot, accounting for soot's feedback to snow and sea ice albedo and emissivity, *J. Geophys. Res.*, *109*, D21,201, doi:10.1029/2004JD004,945, 2004.

Legrand, M., et al. Major 20th century changes of carbonaceous aerosol components (EC, WinOC, DOC, HULIS, carboxylic acids, and cellulose) derived from Alpine ice cores, *J. Geophys. Res.*, *112*(D23S11), doi:10.1029/2006JD008,080, 2007.

Noone, K. J., and A. D. Clarke. Soot scavenging measurements in arctic snowfall, *Atmos. Env.*, *22*(12), 2773–2778, 1988.

Quinn, P. K., et al. Short-lived pollutants in the Arctic: Their climate impact and possible mitigation strategies, *Atmos. Chem. Phys.*, *8*, 1723–1735, 2008.

Warren, S. G. Impurities in snow: effects on albedo and snowmelt, *Annals of Glaciology*, *5*, 177–179, 1984.

Warren, S. G., and R. E. Brandt. Optical constants of ice from the ultraviolet to the microwave: A revised compilation, *In Press in J. Geophys. Res.*, 2008.
Warren, S. G., and A. D. Clarke. Soot in the atmosphere and snow surface of Antarctica, *J. Geophys. Res.*, *95*, 1811–1816, 1990.
Warren, S. G., and W. J. Wiscombe. A model for the spectral albedo of snow. II: Snow containing atmospheric aerosols, *J. Atmos. Sci.*, *37*, 2734–2745, 1980.
Watson, A. Y., and P. A. Valberg. Carbon black and soot: Two different substances, *Am. Ind. Hyg. Assoc. J.*, *62*, 218–228, 2001.
Zender, C. S. Global climatology of abundance and solar absorption of oxygen collision complexes, *J. Geophys. Res.*, *104*(D20), 24,471–24,484, 1999.
Zender, C. S., and J. Talamantes. Solar absorption by Mie resonances in cloud droplets, *J. Quant. Spectrosc. Radiat. Transfer*, *98*(1), 122–129, doi:10.1016/j.jqsrt.2005.05.084, 2006.

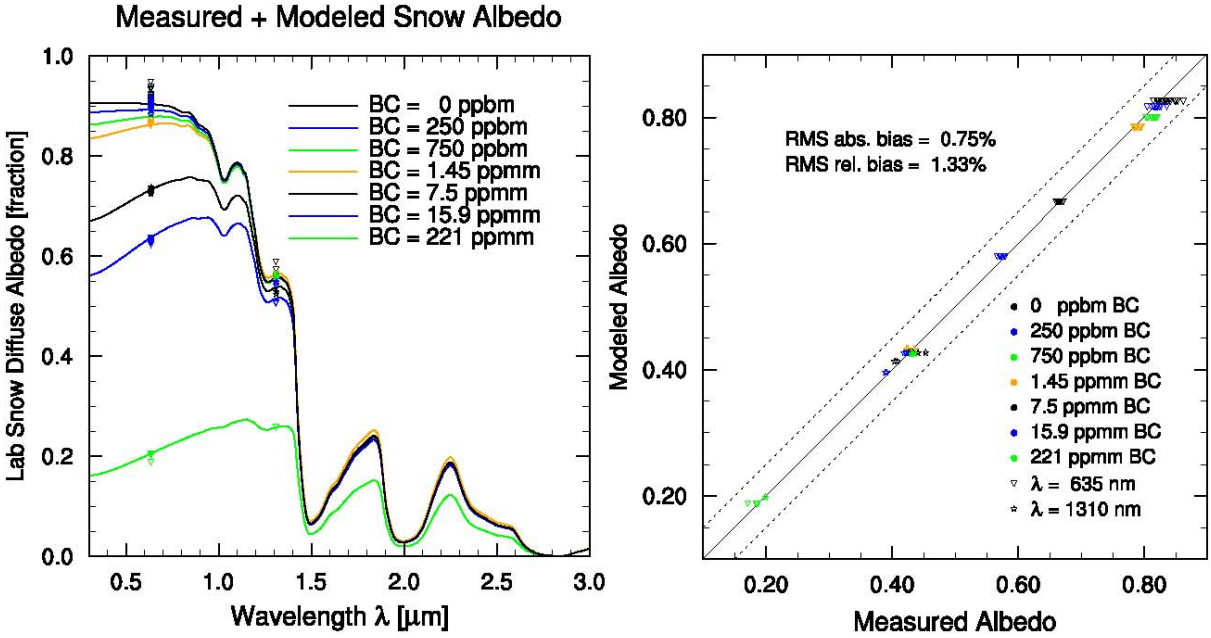

Figure 1. Measured and modeled snowpack reflectance for varying soot (BC) concentration.

Remote sensing of Black carbon at snow and glacier ice surfaces – First results of a modelling approach

R. Solberg[1], C. E. Bøggild[2], A. J. Hodson[3], H. Koren[1], S. Ø. Larsen[1], Ø. D. Trier[1], B. Aamaas[2]
[1]Section for Earth Observation, Norwegian Computing Center, Oslo, Norway; [2]The University Centre in Svalbard (UNIS), Longyearbyen, Norway; [3]Department of Geography, University of Sheffield, Sheffield, England

In 2008–2009, the first phase of the European Space Agency/Norwegian Space Centre PRODEX *Black carbon* project for developing an approach using earth observation for Black carbon monitoring is carried out in Svalbard. The overall objective is to determine whether the Black carbon content of snow and glacier surfaces can be retrieved from satellite data. The project includes efforts to determine the main spectral properties of Black carbon in snow and ice in the Arctic/Svalbard and to determine whether there is sufficient information (signal) in relevant satellite data in order to be successful in retrieval of Black carbon concentrations.

The feedback processes and the high reflectance of the Arctic give a strong impact from Black carbon, despite that only around 10–20% of the global Black carbon emissions end up here (Koch et al. 2007; Flanner, Zender and Randerson 2007; Hansen and Nazarenko 2004). However, an ignored effect so far is the long-term effect of Black carbon on glaciers. Due to downward movement of accumulated snow on glaciers in combination with the ice flow, Black carbon will become entrained in the glaciers and will eventually melt free many years later further down in the melt zone of the same glacier. Black carbon will accordingly accumulate on the ice surface and will thereby contribute to surface darkening. This darkening enhances the melting and contributes to thinning of the arctic glaciers. The magnitude of this enhanced melting is not known presently. But due to ice flow the long-term effect is likely significant and well beyond termination of human Black carbon emission.

Three field sites (glaciers) are studied so far in the project: Longyearbreen, Grønfjordbreen and Eidembreen. Simultaneous satellite and field measurements are carried out a few times during the spring and summer, and possibly combined with additional information from the area, in order to obtain a better picture of what causes the temporal changes in surface albedo.

In each field campaign, a set of spectral reflectance samples are taken. Samples are also collected for material compositional analysis in a laboratory, i.e. determining the fractions of Black carbon, organic material and lithogenetic material. In order to improve the understanding of the evolution on the snow and ice surfaces, an automatic time-lapse camera was set up for taking daily pictures of a glacier surface during the spring and summer period.

The most relevant satellite data are Terra MODIS and ENVISAT MERIS. Supplemental sources could be NOAA AVHRR and ENVISAT AATSR. MODIS data (of 250 and 500 m pixel size) and MERIS data (of 300 m pixel size) are regularly downloaded from data providers.

Two sites have been chosen for satellite measurements of snow, one on each side of the large fjord Isfjorden. One is on Grønfjordbreen south of Barentsburg and the other on Eidembreen north of Isfjorden, The distance between the two sites is about 60 km. The two sites should

have about the same local climate. They are situated between 300 and 400 m above sea level, and both have a small gradient facing towards north, though somewhat more westerly on Eidembreen. With normal conditions without local aerosol sources, one should expect the snow reflectance to be quite similar at the two sites.

One of the applications of these sites is for satellite snow albedo algorithm development, calibration and validation. Soot concentrations are periodically quite large in the Grønfjordbreen area, as around other coal mines in Svalbard. This situation enables more controlled satellite data sensitivity studies of a large range of soot concentrations for field and satellite measurements. On the other side, Eidembreen should hardly be affected of local soot, and therefore functions as a reference site for the satellite measurements.

The satellite-measured top-of-atmosphere (TOA) reflectance values of the two sites are supposed to increase during the spring due to increasing solar elevation. So they do in our observations from the 2008 season, but they start to decrease at the end of the period. This may be caused by melting snow. Without impurities, the temporal development of the TOA reflectance should be quite similar for the two sites. The measured values have been calibrated by subtracting the minimum value in each image. The differences in absolute values and relative to the value on Eidembreen have then been calculated. The values at Eidembreen increase until 12 June and then start decreasing. At Grønfjordbreen the top is reached already 24 May. This could indicate that more impurities at Grønfjordbreen affect the albedo as measured from the satellite. The values at Grønfjordbreen then decrease more than at Eidembreen, and the difference is increasing. One explanation is an increasing amount of impurities in the snow at Grønfjordbreen. As no fieldwork took place at these glaciers in 2008, we have repeated the satellite measurements in 2009 together with field measurements. The Black carbon analysis of the field samples is expected to be available by the end of the year.

Glacier ice surfaces have been measured and sampled in the summer seasons of 2008 and 2009. The high variability in dry-mass distribution on the glacier ice surface, as seen by statistical analysis of surface photos and apparent high variability of surface reflectance, calls for an explanation on how impurities collect and distribute on a melting glacier surface. Many combinations of distributions of cryoconite on the glacier surface are possible. If the airborne impurities were homogenously distributed on the surface, then thickness of the layer would be more than the diameter of each aerosol particle. Since the aerosol particles are opaque this would lead to an albedo of pure cryoconite material, i.e. an albedo of ~4%. At the other extreme we know that the albedo of ice with no impurities is around 60–65%. Many measured surface albedo values deviate from this, and commonly measured abedo values are around 55%. These albedos are significantly higher than for the cryoconite material but lower than for pure ice albedo. Detailed surface observations have revealed that the cryoconite material tend to cluster in nodules which appear to have a spherical shape with a diameter at millimetre scale.

The most likely reason for such nodules to form is bonding by microorganisms living near the nodule surface (see e.g. Hodson et al. 2007). An experiment was performed where microorganisms were removed using potassium hydrogen peroxide. The comparison of albedo from natural cryoconite material and material cleaned from microorganisms did reveal no significant difference. We conclude that the micro organisms ‘hide’ from the ultraviolet radiation of the sun behind the particles and hence cannot be detected spectrally.

A known phenomenon on glacier surfaces is the formation of cryoconite holes. Such holes form when solar radiation does penetrate the ice and absorbs in the cryoconite material inside the ice. A cylindrical or conical shape hole is established upon melt-down of the material. Looking from above (nadir) the optical effect of such a hole is observable. But with increasing angles from zenith the albedo of pure ice becomes dominating. We therefore need to develop a model which can correct for the directional effects associated with cryoconite hole formation.

There are several sources of impurities which reduces the albedo of snow and glacier surfaces. Mineral dust is the major source of aerosols. A small fraction of the aerosols constitute of Black carbon, which due to its strong radiational effect even at small concentrations affects the arctic radiation balance. The aerosols vanish with seasonal snow when it melts away, but they do accumulate on glaciers over time. We have illustrated that storage processes of aerosols controls the ice albedo, and hence the melt rates on glaciers. Therefore, a better understanding of storage/release processes is a key to understand the past, present and future albedo of glaciers.

The results of our initial studies have shown that a model approach is needed to discriminate between various surface material (organic and lithic) and Black carbon. A concept for such a model has been development. A Black carbon retrieval algorithm for glacier ice surfaces will need to include an albedo model taking into account the albedo variability contributors and the associated processes.

If Black carbon retrieval from satellite data is successful for snow and glacier ice surfaces, it will make large-scale monitoring of Black carbon in polar regions possible. This means that concentrations of Black carbon for the first time could be observed as a variable in space and time. Operational Black carbon monitoring will enable improved energy balance modelling, which is of particular importance for modelling climate change effects in polar regions. In most climate models, energy balance processes in these areas are crudely described. Improved climate modelling in polar areas could potentially have a significant impact on long-term climate-change projections on the global scale.

References

Flanner, M.G., Zender, C.S. and Randerson, J.T. Present-day climate forcing and response from Black carbon in snow. *Journal of Geophysical Research* 112, doi:10.1029/2006JD008003, 2007.

Hansen, J. and Nazarenko, V. Soot climate forcing via snow and ice albedos. *Proceedings of the National Academy of Science* 101, 423–428, 2004.

Hodson, A., Anesio, A.M., Ng, F., Watson, R., Quirk, J., Irvine-Fynn, T., Dye, A., Clark, C., McCloy, P., Kohler, J. and Sattler, B. A glacier respires: Quantifying the distribution and respiration CO_2 flux of cryoconite across an entire arctic supraglacial ecosystem. *Journal of Geophysical Research* 112, doi:10.1029/2007JG000452, 2007.

Koch, D., Bond, T.C., Streets, D., Unger, N. and van der Werf, G. Global impacts of aerosols from particular source regions and sectors. *Journal of Geophysical Research*, 112, doi:10.1029/2005JD007024, 2007.

Session 4. Black carbon sources and atmospheric transport

Source attribution of light absorbing aerosol in arctic snow (preliminary analysis of 2008–2009 data)

D. A. Hegg[1], S. G. Warren[1], T. C. Grenfell[1], S. J. Doherty[1,2] and A. D. Clarke[3].
[1]Deptartment of Atmospheric Science, University of Washington, Seattle, Washington, USA; [1]JISAO, University of Washington, Seattle, Washington, USA; [3]School of Ocean and Earth Sciences and Technology, University of Hawaii, Honolulu, Hawaii, USA

A preliminary analysis of recent data on the chemical composition of snow samples obtained in Eastern Siberia (42 samples), Greenland (15) and near the North Pole (4) in 2008, and in the Canadian Arctic in 2009 (132) is presented. In many instances, vertical profiles of the snow composition were obtained (29 cases). All samples are still being analyzed for more chemical species and we therefore emphasize the preliminary nature of the analysis presented here.

The goals of the present analysis are derived from a previous analysis of a more limited data set on snow chemical composition, the samples obtained in 2007 (Hegg et al, 2009). In that study, using receptor modeling (Positive Matrix Factorization), we were able to do a source attribution of the light absorbing aerosol, assumed to be Black carbon, found in the snow. We found that the predominant source of Black carbon in three of the four arctic regions examined (North American Arctic, Western Siberia and Greenland) was biomass burning. For the area around the North Pole, on the other hand, the largest source was industrial pollution. This result was rather surprising and has prompted us to explore the issue further with the current larger data set. Further, the samples obtained in 2007 were nearly all taken from the top ~ 15 cm of the snow pack and hence represented primarily deposition in the spring. It is well known that biomass burning commonly has a peak in activity in the spring and we also wish to address the issue of possible seasonal variation of the relative source strengths by looking at deeper snow samples representative of deposition during the winter and autumn of the previous year. Finally, recent more refined analysis of the aerosol absorption data for the snow aerosol has suggested that Black carbon may not be solely responsible for the observed aerosol light absorption. We have utilized a preliminary partitioning of the light-absorbing aerosol (LAA) into Black carbon and non-black carbon fractions and explored possible differences in the sources of these two species.

Due primarily to the different stages in which the 2008 and 2009 data sets are with respect to the completeness of the chemical analysis, we treat them separately and present first the results from the more completely analyzed 2008 data set. We first examine chemical depth profiles for three of the Eastern Siberian sampling sites for covariation of the various chemical species with the LAA (assumed here to be solely Black carbon). It can be seen that the Black carbon does show substantial vertical variation, equivalent to temporal variability in deposition, with values generally higher near the surface (spring deposition). There is also significant covariation not only with biomass burning markers (e.g., levoglucosan) but also with pollution markers (e.g. NSS sulfate). We next present the results of a PMF analysis of the entire data set. Because the chemical analysis of the samples is still ongoing, we feel it premature to conduct a complete source attribution and confine ourselves to an analysis of the factor loading (both here and for the 2009 data set). This is normally quite indicative of the main sources of a particular constituent, such as LAA, which will be most highly loaded onto the factors representative of its main sources. Four factors, or source profiles, provided the best solution to the inversion problem. Essentially all of the Black carbon was loaded onto a

single factor, which had high loadings of both biomass and pollution markers. We tentatively conclude that the Black carbon is associated with both pollution and biomass burning, the two sources being incompletely resolved at this stage of the analysis. To examine possible seasonality in the Black carbon sources, we next excluded all samples obtained in the top 15 cm of the snow column from the data set and redid the PMF analysis. Once again four factors were found and once again virtually all of the Black carbon was loaded onto a single factor. However, while lightly loaded in general, no significant loading of any biomass marker was found on this factor while significant levels of both Fe and NSS sulfate were present. We tentatively conclude that the Black carbon sources for the winter and spring seasons are predominantly industrial pollution. This contrast with the spring-influenced data is expected but gratifying.

Analysis of the 2009 data set proceeded along similar lines. Chemical depth profiles are first examined for three of the Canadian sites, two in the low (southern) Arctic and one from the high Arctic. The low arctic profiles show high covariance between levoglucosan and both Black carbon and non-black carbon LAA, which are distinct species in this data set. The high arctic profile shows less covariance between the two LAA's and the levoglucosan but the two LAA's show almost identical profiles, the non-BC LAA simply being uniformly displaced to lower concentrations. This suggests that the algorithm used to partition the LAA into non-Black carbon and Black carbon has not been completely successful. We next performed a PMF analysis of the entire data set and found four factors gave the best solution. The factors were somewhat more difficult to interpret than was the case for the 2008 data set, due largely to the relatively modest number of chemical species currently available for analysis. Nevertheless, both the Black carbon and non-black carbon LAA were loaded onto two factors, both of which were most likely biomass based. Hence, both LAA's are tentatively associated with biomass burning. However, attribution of both LAA components to the same sole source may be premature because of the apparent incomplete deconvolution of the two species. As with the 2008 data set, we next eliminated the near surface samples from the data set and redid the PMF analysis. In this instance, however, no difference was found in the factor results between the two PMF runs. This suggests much reduced seasonality in the LAA sources in Canada (2009) compared to the 2008 Eastern Siberian sites.

On the basis of the above analyses, we make the following tentative conclusions.
The new data sets are consistent with the 2007 data set in suggesting that biomass combustion is the main source of LAA in the arctic snow pack.

There is some evidence from the PMF analysis of the 2008 Eastern Siberian data set that there is in fact some seasonality to the relative source strengths of the LAA sources, with the biomass source preeminent in the spring but pollution more important in the winter and fall. The analysis of the 2009 Canadian data set suggests that Black carbon and non-black carbon LAA have similar sources but this conclusion is compromised by the further suggestion that the two LAA constituents have not been completely deconvoluted in the analysis.

Future work will entail completion of the chemical analysis of both the 2008 and 2009 data sets, fresh PMF model runs with these complete data sets followed by a full source attribution. Comparison of the source profiles between the 2007, 2008 and 2009 data sets will be undertaken to assess the feasibility of combining all the data into a single analysis. Receptor modeling with other models than PMF (e.g., UNMIX and ME2) will be explored.

References

Hegg, D. A., S. G. Warren, T. C. Grenfell, S. J. Doherty, T. V. Larson, and A. D. Clarke. Source Attribution of Black carbon in arctic snow. *Environ*. *Sci*. *Technol*., 43, 4016–4021, 2009.

The importance of aging for regional transport of Black carbon to the Arctic

M. T. Lund[1] and T. K. Berntsen[1,2]
[1]CICERO Center for International Climate and Environmental Research, Oslo, Norway;
[2]Department of Geosciences, University of Oslo, Oslo, Norway

Black carbon (BC) aerosols affect climate through absorption of direct and reflected solar radiation, through impact on cloud cover and formation and by reducing the albedo of snow and ice after deposition onto these surfaces. Most BC particles are hydrophobic, i.e. water insoluble, when emitted. Since the main sink of BC is wet deposition, the transfer from hydrophobic to hydrophilic mode, i.e. aging, is a crucial parameter for determining the lifetime, and hence the distribution and transport, of the particles. Aging occurs through condensation of sulphuric and nitric acid onto the aerosols, through coagulation with soluble species and through oxidation (Croft et al., 2005). The aging time thus varies seasonally and regionally depending among other on the availability of such soluble species and on local atmospheric conditions.

Many atmospheric models currently account for BC aging using a constant transfer from hydrophobic to hydrophilic mode. This study compares two different parameterizations of BC aging in the chemical transport model Oslo CTM2. In the original parameterization (abbreviated OP), only total mass of BC is included and BC aging is represented by a constant transfer of 24% per day to hydrophilic mode (Maria et al., 2004). This equals a constant aging time of ~4 days. The second parameterization is a microphysical module called M7, which is described in detail in Vignati et al. (2004) and was recently included in the CTM2. M7 includes aerosol size distribution and particle interaction and thus allows for the formation of mixed aerosols. Aging and growth of BC particles occur through condensation and coagulation with other soluble species. Hence, the aging time can now vary in time and space. The effect on lifetime, distribution and transport of BC to the Arctic with the M7 compared to OP is studied.

The Oslo CTM2 is an offline global, 3-dimensional model driven by meteorological data from ECMWF. For this study, the model was run with a horizontal resolution of 2.8° × 2.8° and 40 vertical layers up to approximately 10hPa. The time period was January 2005 to June 2006, using the first six months as spin-up. BC emissions are from Bond et al. (2004) for fossil fuel and biofuel use and from GFED (Randerson et al., 2007) for biomass burning. A routine for modelling the deposition of BC on snow and ice (Rypdal et al., 2009) was included in the model. For both parameterizations, full simulations with all emissions and simulations with emissions from four separate source regions (Europe, China, North America and Russia) were performed.

Results from the simulations with full emissions reveal that using M7 leads to an increase, compared to OP, in the annual mean near-surface concentration and the zonally averaged column burden of BC at high latitudes, while there is a decrease in lower latitudes. Furthermore, the high-latitude increase occurs mainly during winter and fall. Wet and dry removal and transport is unchanged, so the difference must be attributed to a change in aging time. The increased concentrations at high latitudes is presumably due to the lack of solar radiation required to produce sulphuric acid through the gas-phase reaction $OH+SO_2 \rightarrow H_2SO_4$, which is the only sulphuric acid contributing to the coating of BC aerosols in M7.

Less sulphuric acid results in a slower aging and longer lifetime, and thus to these higher atmospheric concentrations.

The amount of BC in snow and ice shows high variability with maximum concentrations of a few μg g^{-1} close to source regions and in the order of 40 ng g^{-1} over much of Central Asia, Siberia and North America. Above 70°N concentrations are below 10 ng g^{-1} over large areas. Using the M7 module leads to a reduction in the amount of BC in snow and ice at the most northern latitudes compared to OP.

Looking at the regional contributions of fossil fuel plus biofuel BC to the total BC burden north of 65°N with OP, we find that BC originating in Europe is most important, followed by BC from China. Contributions from Russia and North America are smallest. If we look at the burdens in different altitude intervals, we find that fossil fuel plus biofuel BC from emissions in Europe contribute most to the total burden in the lower and middle troposphere. In the upper troposphere, contributions from China are higher. There is no clear seasonal variability when OP is used. Simulations with M7 show very different results. There is now a seasonal pattern in the contributions of BC (fossil fuel plus biofuel) from Europe and Russia to total BC burden north of 65°, with a strong maximum during winter. The contributions are also higher than in the case of OP, especially for Russia, where contributions now almost equal those of BC from Europe. During spring and summer the contribution to burden from these two regions is reduced with the M7. Other studies (Shindell et al., 2008; Skeie et al., this report) have shown that there is a discrepancy between modelled and measured atmospheric BC. Most models strongly underestimate BC at several stations in the Arctic, especially during winter, and the seasonal pattern in the measurements is not captured. Results from the M7 indicate that the treatment of aging might account for at least part of this. Contributions to total BC burden from emissions in China are reduced throughout the year with M7 and there is little seasonal variation. This seems reasonable since the region has relatively constant solar radiation and high SO_2 emissions.

Using the M7 module thus reveals a strong seasonal and regional variability in BC aging time with slower aging during winter in high latitudes due to lack of solar radiation and faster aging in lower latitudes compared to OP. The aging time ranges from 6 days for BC from Russia in January to 1 day for BC from Europe in July. For BC from China, the aging time is almost constant at approximately 1 day. This is significantly different from the constant aging time (~4 days) in OP. The change in aging time also impacts the percentage contribution of BC (fossil fuel plus biofuel) from the different regions to total BC in snow and ice. Except for closest to the source, the contribution from BC from China is reduced with M7 relative to OP, as more BC is removed earlier with a faster aging. Meanwhile, the Russian contribution increases over large areas at the most northern latitudes.

Some uncertainties related to M7 concern the assumption that all BC is emitted as hydrophobic (compared to 20% hydrophilic and 80% hydrophobic in OP) and the possibility that species such as OC and nitric acid also could contribute to the coating of the BC aerosols. Furthermore, using the microphysical module significantly increases the computer resources required. Further comparison with BC measurements can also improve the evaluation of the parameterizations. However, the M7 is physically more realistic than OP and captures a seasonal and regional variation aging time consistent with theoretical considerations.

References

Bond, T. C., Streets, D. G., Yarber, K. F., Nelson, S. M., Woo, J. H. and Klimont, Z. A technology-based global inventory of black and Organic carbon emissions from combustion. *Journal of Geophysical Research–Atmospheres. 109(D14)*, 2004.

Croft, B., Lohmann, U. and von Salzen, K. Black carbon ageing in the Canadian Centre for Climate modelling and analysis atmospheric general circulation model. *Atmospheric Chemistry and Physics. 5*, 1931–1949, 2005.

Maria, S. F., Russell, L. M., Gilles, M. K. and Myneni, S. C. B. Organic aerosol growth mechanisms and their climate-forcing implications. *Science. 306(5703)*, 1921–1924, 2004.

Randerson, J. T., van der Werf, G. R., Giglio, L., Collatz, G. J. and Kasibhatla, P. S. Global Fire Emissions Database, Version 2 (GFEDv2.1). Data set. Available on-line [http://daac.ornl.gov/] from Oak Ridge National Laboratory Distributed Active Archive Center, Oak Ridge, Tennessee, U.S.A, 2007.

Rypdal, K., Rive, N., Berntsen, T. K., Klimont, Z., Mideksa, T. K., Myhre, G. and Skeie, R. B. Costs and global impacts of Black carbon abatement strategies. *Tellus Series B–Chemical and Physical Meteorology. 61(4)*, 625–641, 2009.

Shindell, D. T., Chin, M., Dentener, F., Doherty, R. M., Faluvegi, G., Fiore, A. M., Hess, P., Koch, D. M., MacKenzie, I. A., Sanderson, M. G., Schultz, M. G., Schulz, M., Stevenson, D. S., Teich, H., Textor, C., Wild, O., Bergmann, D. J., Bey, I., Bian, H., Cuvelier, C., Duncan, B. N., Folberth, G., Horowitz, L. W., Jonson, J., Kaminski, J. W., Marmer, E., Park, R., Pringle, K. J., Schroeder, S., Szopa, S., Takemura, T., Zeng, G., Keating, T. J. and Zuber, A. A multi-model assessment of pollution transport to the Arctic. *Atmospheric Chemistry and Physics. 8(17)*, 5353–5372, 2008.

Vignati, E., Wilson, J. and Stier, P. M7: An efficient size-resolved aerosol microphysics module for large-scale aerosol transport models. *Journal of Geophysical Research–Atmospheres. 109(D22)*, 2004.

Black carbon in the atmosphere and deposition on snow, last 130 years.

R.B. Skeie[1], T. Berntsen[1,2], G. Myhre[1], C. A. Pedersen[3], S. Gerland[3], S. Forsström[3] and J. Ström[3]
[1]CICERO Center for International Climate and Environmental Research, Oslo, Norway; [2]Department of Geosciences, University of Oslo, Oslo, Norway; [3]The Norwegian Polar Institute, Tromsø, Norway

The total emissions of Black carbon (BC) from fossil fuel and biofuel combustions have increased almost linearly over the last 150 years, but the regional emissions have a different development. In 1920 the emissions in North America was three times larger than today. Emissions in Europe has decreased since 1960, while China has had a rapid increase in BC emissions over the last decades (Bond et al. 2004). The climate effect of BC emissions is dependent on where the emissions take place (Berntsen et al. 2006), so the changes in the distribution of emissions will affect the climate. Especially in the arctic region, BC may be an important factor and it is argued that cutting the emissions of BC may be important to slow the observed rapid warming in the arctic region (Quinn et al. 2008). In this work the transport of BC in the atmosphere and the deposition of BC on snow covered surfaces for the last 130 years are modelled with the Oslo CTM2 model. Many models have problems in capturing the enhanced winter concentrations in the Arctic (Shindell et al. 2008), including the standard version of the Oslo CTM2 model. In this work we introduce exponential lifetimes for the conversion from hydrophobic to hydrophilic BC aerosols depending on latitude and season. This improves the seasonal cycle of BC at arctic stations.

Oslo CTM2 is an offline chemical transport model using meteorological data from the IFS model at ECMWF. The resolution used is T42 (2.8 x 2.8 degrees) in the horizontal and 60 vertical levels. Advection is calculated by the second order moment scheme (Prather 1986), a scheme that is non-diffusive, has high accuracy and is able to maintain large gradients in the distribution of species. Vertical mixing by convection is based on mass flux data from IFS (Tiedtke 1989), and an-"elevator" principle, surplus or deficit of mass in a columns (Berglen et al. 2004). Turbulent mixing in the boundary layer is treated according to the Holtslag K-profile scheme (Holtslag et al. 1990).

The carbonaceous aerosols scheme used in the Oslo CTM2 is a simple bulk scheme based on (Cooke et al. 1999). Black carbon aerosols are divided into hydrophilic (water-soluble) and hydrophobic (non soluble) aerosols. 80% of the BC emissions are assumed to be hydrophobic and the remaining fraction hydrophilic. The hydrophobic aerosols are aged (oxidized or coated by hydrophilic compounds) and become hydrophilic. The conversion from hydrophobic to hydrophilic aerosols is often treated with a constant exponential lifetime (Cooke et al. 1999). When using a constant conversion rate, the enhanced concentrations in the Arctic during winter (Eleftheriadis et al. 2009; Sharma et al. 2006) were not reproduced. In this work we introduce exponential lifetimes depending on latitude and season. The exponential lifetimes are estimated based on simulations with the full tropospheric chemistry version of Oslo CTM2 with the M7 microphysical module (Vignati et al. 2004). This allows for interaction between aerosols that determines if the aerosols are hydrophilic or hydrophobic. Simulations using this version of Oslo CTM2 with regional emissions are done and lifetimes are calculated (Lund and Berntsen, this report). Based on these simulations and corresponding emissions, latitudinal and seasonal exponential lifetimes are estimated. The values ranging from 5 days during winter and 1.5 during summer at high latitudes. At low

latitudes and in the southern hemisphere 1.5 days are chosen for all seasons. The aerosols are removed from the atmosphere by dry or wet deposition. Dry deposition of hydrophilic aerosols is calculated with a deposition velocity of 0.025 cm/s over land and 0.2 over ocean. For hydrophobic aerosols the deposition velocity is 0.025 cm/s over both land and ocean. Hydrophilic aerosols are removed by wet deposition. For large scale precipitation 100% solubility is assumed in water clouds, and 5% for ice clouds. For convective precipitation 100% solubility is assumed. The aerosols are removed according to the fraction of water content of the cloud removed by precipitation.

The Oslo CTM2 model is extended by a simple routine for calculating the BC concentration in snow (Rypdal et al. 2009). Data on snow fall, melt and evaporation from ECMWF are used to generate and remove snow layers in each grid box. In these snow layers the amounts of deposited BC are stored, and concentration of BC in each snow layer is calculated.

The period 2000 until present is modelled using real time meteorological data. Fossil fuel emission data used are the year 2000 data from Bond (2004) except for the Asian region where REAS emissions (Ohara et al. 2007) are used. For biomass burning BC emission the GFED data set is used (van der Werf et al. 2006).

For the period 1870–2000, time slice simulations are done every 10^{th} year. The period is simulated with constant meteorological data for the year 2000–2001. The emission data used is from Bond (2004) for fossil fuel and biofuel, and data from Ito and Penner (2005) for open biomass burning.

The introduction of conversion rates from hydrophobic to hydrophilic aerosols depending on season and latitude improved the simulation of the arctic haze at Barrow and Zeppelin station. Although for the spring months, the model underestimates the concentrations. The model capture the pollution episode in April-May 2006 (Stohl et al. 2007) at the Zeppelin station, although not as high concentrations as observed. This episode was related to biomass burning, and for the modelling we use monthly mean emission data. This may be one reason for the underestimation.

During the years 2006–2008, the people at the Norwegian Polar Institute have done several measurements of soot in snow in the arctic regions. The model results are compared to the observations done in spring 2007 close to Ny-Ålesund. There is large spread in the observations, and the model results lie in the range of the measurements.

The modelled historical global mean BC burden has increased over the historical period with approximately equal share of fossil fuel and biofuel BC aerosols and aerosols from biomass burning. But north of 65 degrees, the burden has decreased since 1960, and biomass burning had a minor importance using the chosen biomass burning emissions data in this study.

The model results are compared with BC concentrations in the D4 ice core from Greenland (McConnell et al. 2007). From the model results the concentrations are largest around 1920, as in the ice core. The absolute numbers from the model are lower than from the ice core record and we do not capture the sharp decline in the concentrations after 1950. Our simulations are done with constant meteorology. The variability in the annual concentration at the D4 location is large if we look at the simulations for the last 7 years which are run with real time meteorology. There are a variability of +/- 30 % due to transport and annual

variability in biomass emission data. The concentration in the 2001 simulation was in the lower range of the last 7 years.

Since the spatial distribution of BC emissions has changed, the variability may be larger for the historical concentrations than for the current years. For the historical simulations we choose to run the time slice simulations with year 2000–2001 meteorology. Year 2000–2001 was years with low NAO index while the years around 1930 had high NAO-index. Therefore we did a test with 2006–2007 meteorology, years with high NAO index, and 1930 emissions. When using 2006–2007 meteorology with 1930 emissions the burden in snow at the D4 location increased by 10% compared to the run with 2000–2001 meteorology. In addition, the snow accumulation was less in 2006–2007 than 2000–2001 leading to an increase in the concentration by 22%, compared to the 8% increase in the concentration from year 2001 to 2007 in the real time simulation.

From the simulations with regional emissions Northern America was responsible for more than half of the BC deposited in the snow at the D4 location in 1930. But more interesting for the climate effect is the contribution from regions to the whole Arctic. In 1930 Russia and Western Europe was the largest contributors to BC in snow north of 65 degrees, compared to the Greenland ice core where North America was the main contributor.

Allowing the aging times to vary with season and latitude improves agreement with observations of BC in the air in the Arctic. The observed BC-maximum in snow on Greenland during the 1920s is reproduced by the model, but slower reduction thereafter compared to the observations. The D4-record from Greenland is not representative for BC in snow and ice for the whole arctic region due to larger influence of non-North American source regions. In the whole arctic region (north of 65 degrees) the BC burden in the atmosphere reached its maximum around year 1960.

References

Berglen, T. F., Berntsen, T. K., Isaksen, I. S. A. and Sundet, J. K. A. global model of the coupled sulfur/oxidant chemistry in the troposphere: The sulfur cycle, *Journal of Geophysical Research–Atmospheres*, *109* D19, 2004.

Berntsen, T., Fuglestvedt, J., Myhre, G., Stordal, F. and Berglen, T. F. Abatement of greenhouse gases: Does location matter?, *Climatic Change*, *74* 4, 377–411, 2006.

Bond, T. C., Streets, D. G., Yarber, K. F., Nelson, S. M., Woo, J. H. and Klimont, Z. A technology-based global inventory of black and Organic carbon emissions from combustion, *Journal of Geophysical Research–Atmospheres*, *109* D14, 2004.

Cooke, W. F., Liousse, C., Cachier, H. and Feichter, J. Construction of a 1 degrees x 1 degrees fossil fuel emission data set for carbonaceous aerosol and implementation and radiative impact in the ECHAM4 model, *Journal of Geophysical Research–Atmospheres*, *104* D18, 22137–22162, 1999.

Eleftheriadis, K., Vratolis, S. and Nyeki, S. Aerosol Black carbon in the European Arctic: Measurements at Zeppelin station, Ny-Alesund, Svalbard from 1998–2007, *Geophysical Research Letters*, *36*, 2009.

Holtslag, A. A. M., Debruijn, E. I. F. and Pan, H. L. A high-resolution air-mass transformation model for short-range weather forecasting, *Monthly Weather Review*, *118* 8, 1561–1575, 1990.

Ito, A. and Penner, J. E. Historical emissions of carbonaceous aerosols from biomass and fossil fuel burning for the period 1870–2000, *Global Biogeochemical Cycles*, *19* 2, 14, 2005.

McConnell, J. R., Edwards, R., Kok, G. L., Flanner, M. G., Zender, C. S., Saltzman, E. S., Banta, J. R., Pasteris, D. R., Carter, M. M. and Kahl, J. D. W. 20th-century industrial Black carbon emissions altered arctic climate forcing, *Science*, *317* 5843, 1381–1384, 2007.

Ohara, T., Akimoto, H., Kurokawa, J., Horii, N., Yamaji, K., Yan, X. and Hayasaka, T. An Asian emission inventory of anthropogenic emission sources for the period 1980–2020, *Atmospheric Chemistry and Physics*, *7* 16, 4419–4444, 2007.

Prather, M. J. Numerical advection by conservation of 2nd-order moments, *Journal of Geophysical Research–Atmospheres*, *91* D6, 6671–6681, 1986.

Quinn, P. K., Bates, T. S., Baum, E., Doubleday, N., Fiore, A. M., Flanner, M., Fridlind, A., Garrett, T. J., Koch, D., Menon, S., Shindell, D., Stohl, A. and Warren, S. G. Short-lived pollutants in the Arctic: their climate impact and possible mitigation strategies, *Atmospheric Chemistry and Physics*, *8* 6, 1723–1735, 2008.

Rypdal, K., Rive, N., Berntsen, T. K., Klimont, Z., Mideksa, T. K., Myhre, G. and Skeie, R. B. Costs and global impacts of Black carbon abatement strategies, *Tellus Series B–Chemical And Physical Meteorology*, *61* 4, 625–641, 2009.

Sharma, S., Andrews, E., Barrie, L. A., Ogren, J. A. and Lavoue, D. Variations and sources of the equivalent Black carbon in the high Arctic revealed by long-term observations at Alert and Barrow: 1989–2003, *Journal Of Geophysical Research–Atmospheres*, *111* D14, 2006.

Shindell, D. T., Chin, M., Dentener, F., Doherty, R. M., Faluvegi, G., Fiore, A. M., Hess, P., Koch, D. M., MacKenzie, I. A., Sanderson, M. G., Schultz, M. G., Schulz, M., Stevenson, D. S., Teich, H., Textor, C., Wild, O., Bergmann, D. J., Bey, I., Bian, H., Cuvelier, C., Duncan, B. N., Folberth, G., Horowitz, L. W., Jonson, J., Kaminski, J. W., Marmer, E., Park, R., Pringle, K. J., Schroeder, S., Szopa, S., Takemura, T., Zeng, G., Keating, T. J. and Zuber, A. A multi-model assessment of pollution transport to the Arctic, *Atmospheric Chemistry and Physics*, *8* 17, 5353–5372, 2008.

Stohl, A., Berg, T., Burkhart, J. F., Fjaeraa, A. M., Forster, C., Herber, A., Hov, O., Lunder, C., McMillan, W. W., Oltmans, S., Shiobara, M., Simpson, D., Solberg, S., Stebel, K., Strom, J., Torseth, K., Treffeisen, R., Virkkunen, K. and Yttri, K. E. Arctic smoke – record high air pollution levels in the European Arctic due to agricultural fires in Eastern Europe in spring 2006, *Atmospheric Chemistry and Physics*, *7*, 511–534, 2007.

Tiedtke, M. A comprehensive mass flux scheme for cumulus parameterization in large-scale models, *Monthly Weather Review*, *117* 8, 1779–1800, 1989.

van der Werf, G. R., Randerson, J. T., Giglio, L., Collatz, G. J., Kasibhatla, P. S. and Arellano Jr, A. F. Interannual variability in global biomass burning emissions from 1997 to 2004, *Atmos. Chem. Phys.*, *6* 11, 3423–3441, 2006.

Vignati, E., Wilson, J. and Stier, P. M7: An efficient size-resolved aerosol microphysics module for large-scale aerosol transport models, *Journal of Geophysical Research–Atmospheres*, *109* D22, 2004.

Session 5. Climate modeling

Climate response and efficacy of snow albedo forcing in the HadGEM2-AML climate model

N. Bellouin[1] and O. Boucher[1]
[1]Met Office Hadley Centre, Exeter, United Kingdom

The presence of Black carbon in lying snow can reduce the albedo of the snow surface (Warren and Wiscombe, 1980) and cause a perturbation to the Earth's radiation budget (Clarke and Noone, 1985) by enhancing the absorption of shortwave radiation at snow surfaces. The induced warming is likely to increase the rate of snow melt, which can expose the less reflective underlying surface and decrease the surface albedo further. Here, we present the results of an idealised experiment using the HadGEM2-AML climate model where land snow albedo has been decreased by 0.05. The resulting radiative forcing at the top of the atmosphere is +0.28 Wm^{-2} and global near-surface temperature warms by 0.72 K. Compared to a doubling of CO_2 concentration, this perturbation to snow albedo has a climate efficacy of 2.6. This large value stems from the large efficiency of snow albedo forcing to warm high latitudes, with a relatively larger impact on sea-ice area and snowpack as compared to the CO_2 forcing. These results provide some support to the idea that emission reduction of Black carbon can bring some benefits to mitigate climate change in Arctic and snow regions.

The Hadley Centre general circulation model HadGEM2 can be configured to couple an atmosphere model (Martin et al., 2006) with a 50-m thermodynamic mixed-layer ocean and sea-ice model (Johns et al., 2006). This configuration is used here for a control and two experiment simulations. The control simulation uses trace gas and aerosol concentrations for 1860. The control CO_2 concentration is 286.2 ppmv. That value is doubled in a first experiment, labelled DCO2, to 572.4 ppmv. The albedo of snow-covered land surfaces is prescribed by default at 0.8. That value is decreased to 0.75 in a second experiment, labelled SNOW. In reality, such a large decrease in albedo would only correspond to the largest concentrations of Black carbon in snow. The albedo of snow-covered sea ice is left unchanged.

Each simulation consists of running the model for 30 years after a common starting point obtained by a calibration simulation for 1860 conditions. The 20-year calibration simulation determines the heat-flux distribution needed for maintaining sea-surface temperatures close to climatological values in a mixed-layer ocean which cannot simulate ocean currents. DCO2 and SNOW experiments take about 10 simulated years to reach an equilibrium beyond which the global-averaged 1.5-m temperature, sea-ice fraction and depth, and net radiative fluxes at the top of the atmosphere do not vary significantly. In the following, averages over the last 20 years of each simulation are used. Although the experiments are used to determine the response to their associated forcing, they cannot provide an estimate of the forcings themselves as the model evolution is affected by feedbacks. We quantify the forcing in an additional 5-year atmosphere-only simulation where the model evolution is made independent of the imposed forcing by calling the radiation code twice, first with the forcing mechanism included, then with the control configuration. This last state is used for advancing the model into its next time step.

Decreasing the albedo of snow exerts a radiative forcing that is purely in the shortwave with a global average of +0.28 Wm^{-2}. This global average is relatively small, considering the large

change in snow albedo. Locally, the magnitude of the forcing depends on the duration of snow cover and the amount of solar radiation. In consequence, this radiative forcing displays a strong seasonality, being maximum during summer over polar regions and during spring over northern continents, and virtually zero during polar winter.

Doubling the CO_2 concentration exerts a forcing of -0.19 Wm^{-2} in the shortwave and +4.02 Wm^{-2} in the longwave, for a net forcing of +3.83 Wm^{-2} measured at the tropopause. The CO_2 radiative forcing has a maximum in the Tropics and is zonally symmetric.

Decreasing snow albedo induces a warming of +0.72 K, and +3.85 K for a doubled CO_2 concentration. North Hemisphere warming is stronger in winter than in summer in both experiments. Figure 1 shows the zonal mean temperature change normalised by the globally averaged forcing for both experiments. The normalised warning in SNOW is significantly stronger than in DCO2. Both show an enhancement of the warming at high latitudes. In addition to the surface albedo feedback discussed below, it is hypothesised that changes in the poleward atmospheric heat transport also contribute to the enhancement. In DCO2, heat is transported from tropical to high-latitude regions. In SNOW, heat remains confined at high-latitudes although the Tropics also warm as poleward heat transport is reduced (Shindell and Faluvegi, 2009).

Table 1 gives the global change with respect to the control simulation in 1.5-m temperature, sea-ice area, and precipitation rate, normalised by the imposed forcing. The climate sensitivity is 2.57 K/(Wm^{-2}) for SNOW and 1.01 K/(Wm^{-2}) for DCO2. The ratio of these two numbers, equal to 2.6, is the efficacy of decreasing snow albedo in HadGEM2-AML. This value is at the lower end of the range of 2.5–4.1 estimated for Black carbon deposition on snow by Flanner et al. (2007) and consistent with Koch et al. (2009) and references therein. This large climate sensitivity is likely to be due to the feedback between climate and surface albedo which is excited stronger by this forcing: the reduction in sea-ice area per unit forcing is 4.1 times larger in SNOW than DCO2 (Table 1). Retreating sea ice exposes the darker ocean surface, leading to more warming. Interestingly, in SNOW sea ice reacts to a remote forcing, as the albedo of snow-covered sea-ice surfaces was not modified.

The water cycle is also affected by warmer temperatures. Both SNOW and DCO2 show an increase in precipitation as warmer conditions increase the surface latent heat flux. With an increase in precipitation rate that is 2.8 times larger, the response in SNOW is again larger than in DCO2. The limit between rain and snow moves toward higher latitudes, although snowfall rates are increased north of that line. Snow melt is also affected by warming. Figure 2 shows seasonal distributions of change in snowmelt rates in SNOW and DCO2. Magnitudes are comparable in both experiments, hinting at a larger efficiency at melting snow per unit forcing in SNOW as the snow albedo forcing is located where it matters most to melt snow, directly on snow surfaces. In northern continents, snow melt first increases in winter and even more strongly in spring, before decreasing in summer and autumn as snow has already melted earlier in the year. Snow melts rapidly at the edges of Greenland during summer.

Two radiative forcing mechanisms have been compared in the Hadley Centre atmosphere/mixed-layer ocean climate model. Reducing the albedo of snow-covered land surfaces by 5% and doubling the CO_2 concentration yield a positive response in near-surface temperature, enhanced at high latitudes. The snow albedo mechanism is more efficient at warming the Earth's climate, with an efficacy of 2.6. This large value is due to the snow albedo forcing being applied in precisely the regions where the strong surface albedo

feedback operates. It is thus more efficient at reducing sea-ice and land-snow areas. The hydrological cycle is also more affected by reducing snow albedo than doubling CO_2, with a disproportionate effect on snow melt.

Mitigating the causes of a reduction in snow albedo, such as deposition of Black carbon on snow, would only address a small component of the radiative forcing of the Earth's climate but is likely to suppress a significant warming in high-latitude regions.

References

Clarke, A.D. and Noone, K.J. Soot in the arctic snowpack: a cause for perturbations in radiative transfer. *Atmos. Env.*, 19, 2045–2053, 1985.

Flanner, M.G., Zender, C.S., Randerson, J.T., and Rasch, P. Present-day climate forcing and response from Black carbon in snow. *J. Geophys. Res.*, 112, D11202, doi:10.1029/2006JD008003, 2007.

Johns, T.C. *et al.* The new Hadley Centre climate model (HadGEM1): Evaluation of coupled simulations. *J. Clim.*, 19, 1327–1353, 2006.

Koch *et al.* Distinguishing aerosol impacts on climate over the past century. *J. Clim.*, 2659–2677, doi:10.1175/2008JCLI2573.1, 2009.

Martin, G.M. *et al.* The physical properties of the atmosphere in the new Hadley Centre Global Environment Model (HadGEM1). Part I: Model description and global climatology. *J. Clim.*, 19, 1274–1301, 2006.

Shindell, D. and Faluvegi, G. Climate response to regional radiative forcing during the twentieth century. *Nature Geoscience*, 2, 294–300, doi:10.1038/ngeo473, 2009.

Warren, S.G. and Wiscombe, W.J. A model for the spectral albedo of snow. II: Snow containing atmospheric aerosols. *J. Atmos. Sci.*, 37, 2734–2745, 1980.

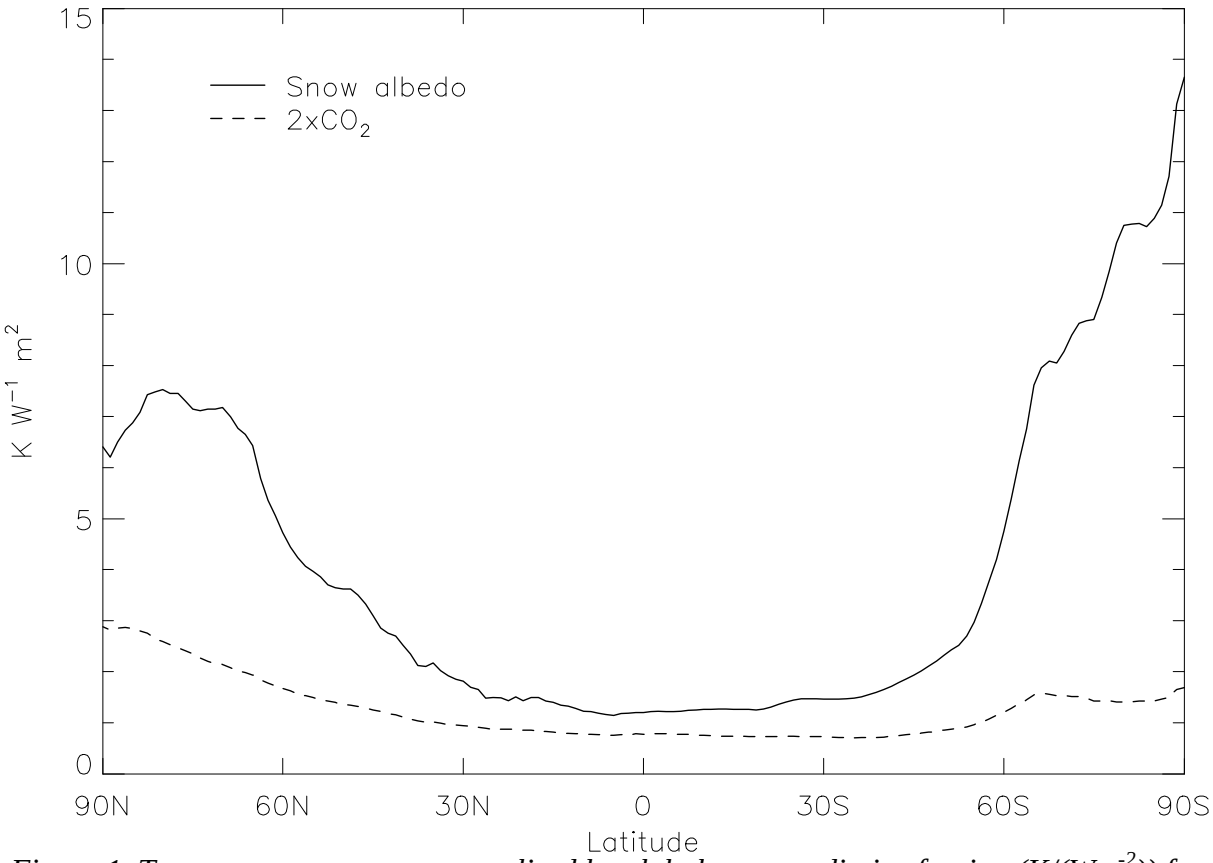

Figure 1. Temperature response normalised by global-mean radiative forcing (K/(Wm^{-2})) for a 0.05 absolute decrease in land snow albedo (solid) and a doubling of CO_2 concentration (dashed).

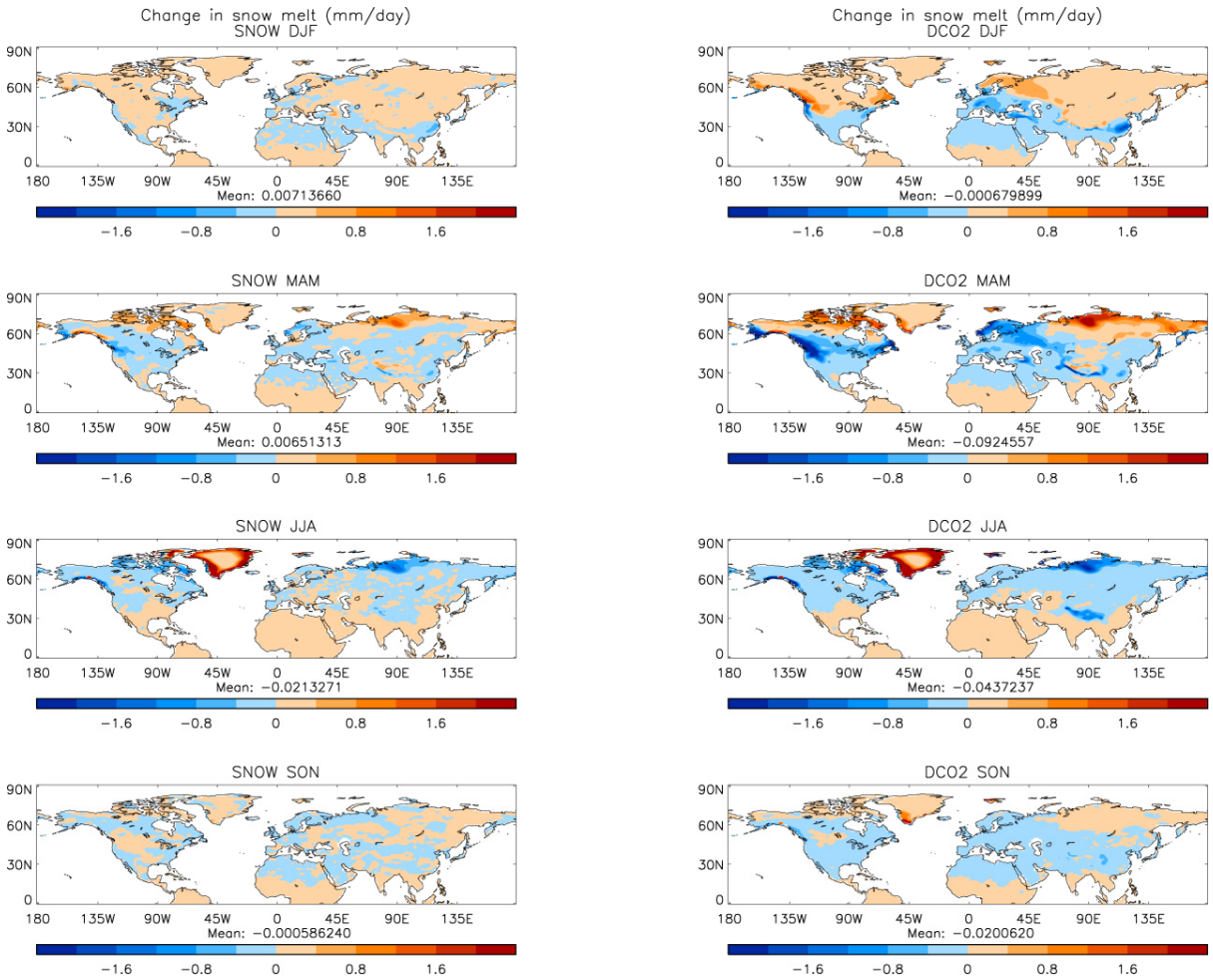

Figure 2. Seasonal change in snow melt rate (mm/day) for a 0.05 absolute decrease in land snow albedo (left) and doubling of CO_2 concentration (right).

Normalised response	**SNOW**	**DCO2**
1.5-m temperature (K/Wm^{-2})	+2.57	+1.01
Sea-ice area (10^6 km^2/Wm^{-2})	-13.9	-3.4
Precipitation rate (10^{-2} mm day^{-1}/Wm^{-2})	+14.0	+5.0

Table 1. Global annual-mean responses normalised by global annual-mean forcing for at 5% decrease in land snow albedo (SNOW) and doubling of CO_2 concentration (DCO2)

Springtime warming and reduced snow cover from carbonaceous particles

M. G. Flanner[1], C. S. Zender[2], P. G. Hess[1,3], N. M. Mahowald[1,3], T. H. Painter[4], V. Ramanathan[5], P. J. Rasch[1]
[1]National Center for Atmospheric Research, Boulder Colorado, USA; [2]University of California, Irvine California, USA; [3]Cornell University, Ithaca New York, USA; [4]University of Utah, Salt Lake City Utah, USA; [5]Scripps Institute of Oceanography, University of California-San Diego, La Jolla California, USA

This is an abridged version of a study published at:
http://www.atmos-chem-phys.org/9/2481/2009/acp-9-2481-2009.html

Boreal spring climate is uniquely susceptible to solar warming mechanisms because it has expansive snow cover and receives relatively strong insolation. Carbonaceous particles can influence snow coverage by warming the atmosphere, reducing surface-incident solar energy (dimming), and reducing snow reflectance after deposition (darkening). We apply a range of models and observations to explore impacts of these processes on springtime climate, drawing several conclusions: 1) Nearly all atmospheric particles (those with visible-band single-scatter albedo less than 0.999), including all mixtures of Black carbon (BC) and organic matter (OM), increase net solar heating of the atmosphere–snow column. 2) Darkening caused by small concentrations of particles within snow exceeds the loss of absorbed energy from concurrent dimming, thus increasing solar heating of snowpack as well (positive net surface forcing). Over global snow, we estimate 6-fold greater surface forcing from darkening than dimming, caused by BC+OM. 3) Equilibrium climate experiments suggest that fossil fuel and biofuel emissions of BC+OM induce 95% as much springtime snow cover loss over Eurasia as anthropogenic carbon dioxide, a consequence of strong snow-albedo feedback and large BC+OM emissions from Asia. 4) Of 22 climate models contributing to the IPCC Fourth Assessment Report, 21 underpredict the rapid warming ($0.64\ ^{\circ}\mathrm{C\ decade}^{-1}$) observed over springtime Eurasia since 1979. Darkening from natural and anthropogenic sources of BC and mineral dust exerts 3-fold greater forcing on springtime snow over Eurasia ($3.9\mathrm{Wm}^{-2}$) than North America ($1.2\mathrm{Wm}^{-2}$). Inclusion of this forcing significantly improves simulated continental warming trends, but does not reconcile the low bias in rate of Eurasian spring snow cover decline exhibited by all models, likely because BC deposition trends are negative or near-neutral over much of Eurasia. Improved Eurasian warming may therefore relate more to darkening-induced reduction in mean snow cover.

To examine surface and top-of-atmosphere (TOA) radiative forcing caused by particles over and within snowpack, we applied the Shortwave Narrowband (SWNB) model (Zender et al., 1997). SWNB utilizes the Discrete Ordinates Radiative Transfer (DISORT) model (Stamnes et al., 1988) and solves for fluxes in 1690 spectral bands from 0.17−5.0 μm. We modify this model to include a single, semi-infinite layer of snow (i.e., thicker than ∼ 20 cm) at the bottom of the atmosphere, thus simulating radiation throughout the atmosphere-snow column. This approach has been adopted in previous studies (Nolin and Dozier, 1993; Aoki et al., 1999; Munneke et al., 2008), and is preferable, in the current context, to methods which prescribe downwelling flux on snowpack as a boundary condition (e.g., Flanner and Zender, 2006). We report spectrally-integrated daily-mean forcings for a range of aerosol single-scatter albedo (SSA) and particle mixing ratio within snow. We prescribe SSA and extinction

optical depth at 500 nm, and scale the spectral distributions of these properties according to Mie properties of sulfate (for SSA 0.9999), water-soluble organic matter (Hess et al., 1998) (for SSA 0.7), and Black carbon (Chang and Charalampopoulos, 1990; Bond and Bergstrom, 2006) (for SSA < 0.7). We estimate fluxes at half-hour resolution for an atmosphere-snow column at 45ºN on April 1, assuming a snowpack effective grain size of 200 µm (representative of fresh or slightly-aged snow). The importance of effective grain size in determining albedo perturbation is discussed in previous studies (Warren and Wiscombe, 1980; Flanner and Zender, 2006; Flanner et al., 2007).

Figure 1 shows clear-sky top-of-atmosphere (TOA) and surface solar radiative forcings as a function of particle single-scatter albedo (SSA) at 500 nm, with identical optical properties applied to particles in the atmosphere and snow. Atmospheric extinction optical depth is fixed at 0.2, but the forcing behavior discussed below remains robust under a doubling or halving of this term. Curves are shown for different values of α, which describes the ratio of particle mixing ratio in snow (kg kg^{-1}) to atmospheric column burden (kg m^{-2}). Surface forcing, in this discussion, represents the combined effect of reduced absorption from atmospheric aerosols and increased absorption from snow darkening.

Several features of Figure 1 are worth noting. First, aerosol mixtures with SSA < 0.999 (co-SSA > 10^{-3}) exert a positive TOA forcing over (thick) snow, even with no particles in the underlying snow (α = 0). The range of positive forcing includes organic matter (Hess et al., 1998), often considered the "scattering" component of carbonaceous aerosol mixtures, as well as weakly absorbing clay minerals like montmorillonite. We note that the range of aerosol SSA producing positive TOA forcing will be reduced over snowpacks thinner than ~ 20cm (Wiscombe and Warren, 1980), as exposure of the underlying surface reduces albedo. The interval between vertical bars "Black carbon" and "organic matter" can be considered a reasonable range of effect for carbonaceous aerosol mixtures over snow, where fossil fuel sources are skewed towards BC and biomass burning sources towards OM (e.g., Andreae and Merlet, 2001). Second, the influence of particles in snow increases TOA forcing for mixtures with co-SSA > 10^{-4} (and slightly decreases forcing for highly scattering mixtures, like pure sulfate with co-SSA ~ 10^{-8}). Third, absorbing aerosols in the atmosphere strongly reduce downwelling surface insolation (curve labeled "dimming"), but the resulting surface forcing (α = 0) is only weakly negative because most of the reduced downwelling radiation would have been reflected by the bright snowpack (e.g, Cess, 1983). Fourth, and perhaps most important, the darkening effect caused by small mixing ratios of particles in snow (α> 0.01) exceeds the reduced absorption from dimming, producing net positive surface forcing. Snow reflectance is easily perturbed because multiple scattering of visible-band photons produces highly actinic flux near the snow surface, enabling very small quantities of particles to absorb a disproportionate amount of radiation (e.g., Warren and Wiscombe, 1980).

References

Andreae, M. O., and P. Merlet. Emission of trace gases and aerosols from biomass burning, *Global Biogeochem. Cycles*, 15 (4), 955–966, 2001.

Aoki, T., T. Aoki, M. Fukabori, and A. Uchiyama. Numerical simulations of the atmospheric effects on snow albedo with a multiple scattering radiative transfer model for the snow–atmosphere system, *J. Meteorol. Soc. Japan*, 77 (2), 595–614, 1999.

Bond, T. C., and R. W. Bergstrom. Light absorption by carbonaceous particles: An investigative review, *Aerosol Sci. Technol.*, 40 (1), 27–67, doi:10.1080/02786820500421521, 2006.

Cess, R. D. Arctic aerosols: Model estimates of interactive influences upon the surface-atmosphere clear-sky radiation budget, *Atmos. Environ.*, 17 (12), 2555–2564, 1983.

Chang, H., and T. T. Charalampopoulos. Determination of the wavelength dependence of refractive indices of flame soot, *Proc. Roy. Soc. London A, Math. and Phys. Sci*., 430 (1880), 577–591, 1990.

Flanner, M. G., and C. S. Zender. Linking snowpack microphysics and albedo evolution, *J. Geophys. Res*., 111, D12208, doi:10.1029/2005JD006834, 2006.

Flanner, M. G., C. S. Zender, J. T. Randerson, and P. J. Rasch. Present day climate forcing and response from Black carbon in snow, *J. Geophys. Res.*, 112, D11202, doi: 10.1029/2006JD008003, 2007.

Hess, M., P. Koepke, and I. Schult. Optical properties of aerosols and clouds: The software package OPAC, *Bull. Am. Meteorol. Soc*., 79 (5), 831–844, 1998.

Munneke, P. K., C. H. Reijmer, M. R. van den Broeke, G. König-Langlo, P. Stammes, and W. H. Knap. Analysis of clear-sky Antarctic snow albedo using observations and radiative transfer modeling, *J. Geophys. Res.*, 113, D17118, doi:10.1029/2007JD009653, 2008.

Nolin, A. W., and J. Dozier. Estimating snow grain size using AVIRIS data, *Remote. Sens. Environ*., 44, 231–238, 1993.

Ramanathan, V., et al. Indian Ocean Experiment: An integrated analysis of the climate forcing and effects of the great Indo–Asian haze, *J. Geophys. Res*., 106 (D22), 28,371–28,398, 2001.

Stamnes, K., S.-C. Tsay, W. Wiscombe, and K. Jayaweera. Numerically stable algorithm for discrete-ordinate-method radiative transfer in multiple scattering and emitting layered media, *Appl. Opt*., 27 (12), 2502–2509, 1988.

Warren, S., and W. A. Wiscombe. A model for the spectral albedo of snow. II: Snow containing atmospheric aerosols, *J. Atmos. Sci*., 37, 2734–2745, 1980.

Wiscombe, W. J., and S. G. Warren. A model for the spectral albedo of snow. I: Pure snow, *J. Atmos. Sci*., 37, 2712–2733, 1980.

Zender, C. S., B. Bush, S. K. Pope, A. Bucholtz, W. D. Collins, J. T. Kiehl, F. P. J. Valero, and J. Vitko, Jr. Atmospheric absorption during the Atmospheric Radiation Measurement (ARM) Enhanced Shortwave Experiment (ARESE), *J. Geophys. Res.*, 102 (D25), 29,901–29,915, 1997.

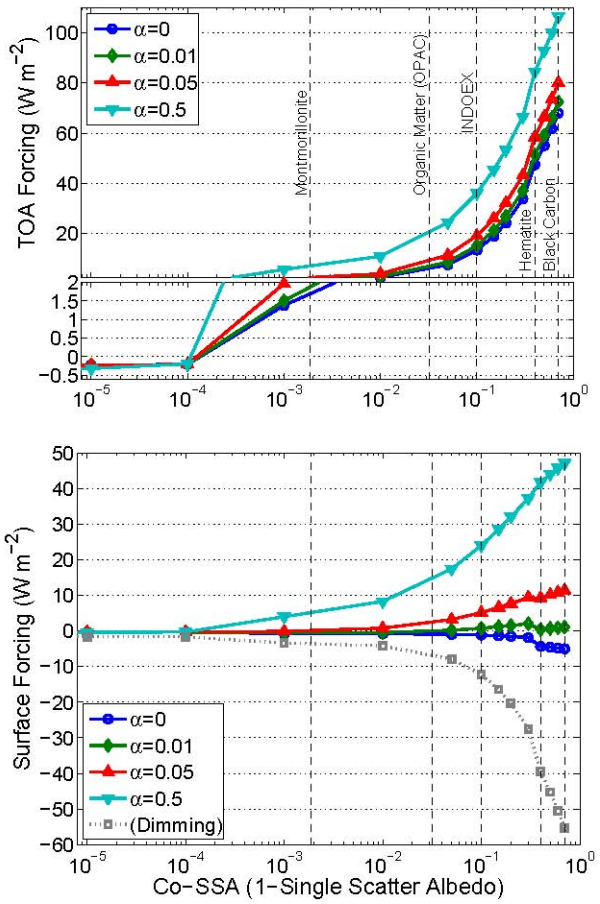

Figure 1: Daily-mean (top) top-of-atmosphere and (bottom) surface changes in net solar power (forcing) as a function of single-scatter albedo complement (1-SSA) at 500 nm. Extinction optical depth of the atmospheric aerosol is fixed at 0.2 and the environment represents a clear-sky atmosphere overlying snowpack with effective grain size of 200 μm on April 1 at 45ºN. Curves are shown for different values of α, the ratio of particle mixing ratio in snow to atmospheric column burden. Forcings represent the combined influence of particles in the atmosphere and snow. For reference, the change in downwelling surface insolation ("Dimming") is also depicted. Vertical lines depict common SSA values of Black carbon, organic matter, and that measured during the Indian Ocean Experiment (INDOEX) (Ramanathan et al., 2001). Also shown are SSA values of strongly and weakly absorbing components of dust aerosols

BC-albedo effects on climate in the GISS model

D. Koch[1], G. Schmidt[2], I. Alienov[2], D. Shindell[2], G. Faluvegi[2], R. Ruedy[3], S. Menon[4], J. McConnell[5], S. Bauer[2], R. Miller[2]
[1]Columbia University, New York, USA; [2]NASA Goddard Institute for Space Studies, New York, USA; [3]Sigma Space Partners, NASA Goddard Institute for Space Studies; New York, USA; [4]Lawrence Berkeley Laboratory, Berkeley, California, USA; [5]Hydrologic Sciences Division, Desert Research Institute, Reno, Nevada, USA

We modeled the climate effects of BC deposition on snow in the GISS model during the 20th century. The climate effects were based on both equilibrium climate experiments with a Qflux ocean for the years 2000 vs 1890 (Koch et al., 2009), and on transient climate experiments for the 20th century from 1880 through 2000 coupled to a model with deep ocean. In both cases the aerosols are online and fully coupled to climate, and the model includes direct, indirect-cloud as well as BC-albedo effects. For both studies, multiple simulations were performed allowing us to distinguish among direct effects, indirect effects and BC-albedo effects on climate. BC emissions in the transient simulation are from Bond et al. (2007). Biomass burning emissions are from GFED where we have scaled these by ½ for tropical burning in 1880 and assumed linear increase to the year 2000; extra-tropical burning is assumed constant throughout the century.

Since we are modeling BC effects, mostly in the Arctic, we have taken some care to compare the model with arctic BC measurements. Model BC surface concentrations and absorption aerosol optical depths are smaller than observed/retrieved in the Arctic, although the GISS model has more BC than most other global models. On the other hand, the GISS model compares fairly well with tropospheric aircraft measurements in the Arctic (Koch et al., 2009b) and with BC deposition measurements (Koch et al., 2009). The BC deposition was tuned to agree with these measurements, by adjusting the fraction of BC removed by frozen precipitation relative to that removed by liquid rain.

The BC albedo scheme in the GISS model (Koch et al., 2009) is based on Warren and Wiscombe's (1985) dependence of snow albedo on BC concentrations in snow. Since this depends on snow grain size, we parameterize snow grain size using surface air temperature and snow age as given by Marshall (1989).

We have also compared the model BC 20th century trends with available measurements. Compared with Greenland ice core records (McConnell et al., 2008), the model BC peaks at the right time (1910s-1920s) but does not peak as high as observed, and does not drop to values as low in one of the cores (ACT2). Model BC deposition in northern Europe peaks in the 1950s, in qualitative agreement with Svalbard BC measurements of Hicks and Isaksson (2006). Compared with BC lake core sediments in the Adirondaks of NY for 1880–2000 (Husain et al., 2008), the model peaks in 1920 as observed and drops to lowest values in recent decades, however the model does not have as much BC as observed from 1950s-1990s. Compared with BC in lake cores in China (Yongming Han, personal communication) the model trends are qualitatively correct in the north but do not rise as much as observed in recent decades on the Tibetan plateau.

Over the century, the GISS model has relatively small BC-albedo forcing, 0.01 Wm^{-2}, however the impact on snow albedo and surface air temperatures (SAT) are fairly large

compared with previous studies (Koch et al., 2009). The mean arctic BC-albedo forcing was largest in the 1950s, so the change from 1880s to 1950s is 0.05 Wm^{-2}; however this forcing decreased from the 1950s to the 1990s, -0.04 Wm^{-2}, as arctic BC has declined during these years. Nevertheless, the 1990s BC-albedo forcing is quite substantial, 0.18 Wm^{-2} in the Arctic, suggesting that there is substantial opportunity to reduce BC effects further in the Arctic. The model indicates that 80% of arctic BC is from fossil fuel and biofuel, and 20% from biomass burning.

We have considered the model's ability to simulate climate (SAT) change during the 20th century by dividing the century into three periods, a strongly warming period from 1890s to 1940s, a stable climate period from 1940s to 1970s and another strong warming period from the 1970s to the 1990s. The GISS model with interactive species does a reasonable job of simulating SAT changes up to the 1970s but does not warm as much as observed during 1970s-1990s. This deficiency may be due to excessive indirect effects at the end of the century, connected to insufficient sulfate decline (in emissions).

The model indicates that the BC-albedo effect contributed 20% of arctic climate warming over the century, 25% during the 1890s-1940s. From the 1970s-1990s the BC-albedo effect decrease actually cooled the Arctic due to decreased BC especially from Europe.

According to the model, the BC-albedo effect caused 20% of Arctic and 35% of global ice/snow cover loss over the century. This effect is strongest early in the century, from the 1890s-1940s it caused 40% of Arctic and nearly all of the global ice/snow loss. From the 1940s-1970s the BC-albedo effect caused all arctic snow/ice loss. From the 1970s-1990s the BC-albedo effect caused increased snow/ice cover by an amount comparable to the net modeled loss due presumably to greenhouse gas warming.

References

Bond, T. C., E. Bhardwaj, R. Dong, R. Jogani, S. Jung, C. Roden, D. G. Streets, and N. M. Trautmann. Historical emissions of black and Organic carbon aerosol from energy-related combustion, 1850–2000, *Global Biogeochemical Cycles*, 21, GB2018, doi:10.1029/2006GB002840, 2007.

Hicks, S., and E. Isaksson, Assessing source areas of pollutants from studies of fly ash, charcoal, and pollen from Svalbard snow and ice, *J. Geophys. Res*., 111, D02113, doi:10.1029/2005JD006167, 2006.

Husain, L., A. J. Khan, T. Ahmed, K. Swami, A. Bari, J. S. Webber, and J. Li. Trends in atmospheric elemental carbon concentrations from 1835 to 2005. *J. Geophys. Res.*, v 113, D1312, doi:10.1029/2007JD009398, 2008.

Koch, D., S. Menon, A. Del Genio, R. Ruedy, I. Aleinov, and G.A. Schmidt. Distinguishing aerosol impacts on climate over the past century. *J. Climate*, 22, 2659–2677, doi:10.1175/2008JCLI2573.1., 2009a.

Koch, D. Evaluation of Black carbon estimations in global aerosol models. *Atmos. Chem. Phys. Disc*., 2009b.

Marshall, S. E. A physical parameterization of snow albedo for use in climate models. Ph.D. thesis, University of Washington, NCAR, and University of Colorado, 161 pp., 1989.

McConnell, J. R., R. Edwards, G. L. Kok, M. G. Flanner, C. S. Zender, E. S. Saltzman, J. R. Banta, D. R. Pasteris, M. M. Carter, J. D. W. Kahl, 20th-Century industrial Black carbon emissions altered arctic climate forcing, *Science* 7, 1381–1384, DOI: 10.1126/science.1144856, 2007.

Warren, S. G., and W. J. Wiscombe, Dirty snow after nuclear war. *Nature*, 313, 467–470, 1985.

Session 6. Mitigation

The task force on short-lived climate forcers under the Arctic Council

B. DeAngelo[1]
[1]*Office of Atmospheric Programs, U.S. Environmental Protection Agency, Washington, USA*

The potential for Black carbon emissions to contribute to climate change is now receiving significant attention in a number of policy areas. How Black carbon emissions may be contributing to climate change in the Arctic in particular has increased the visibility of this issue even more over the past few years. The Arctic Council, a high-level intergovernmental consortium consisting of Canada, Denmark, Finland, Iceland, Norway, the Russian Federation, Sweden, and the U.S., agreed upon a declaration 29 April 2009 in Tromsø, Norway, stating they, among other things, would:

> *"Decide to establish a task force on short-lived climate forcers to identify existing and new measures to reduce emissions of these forcers and recommend further immediate actions that can be taken and to report on progress at the next Ministerial meeting."*

The next Arctic Council Ministerial meeting referred to will take place in the spring of 2011. Black carbon is one of the main pollutants to be addressed by the task force, but methane and tropospheric ozone will be addressed as well. The task force will be focused on mitigation issues (not original scientific research) and will therefore need to cooperate with and leverage information from AMAP (Arctic Monitoring and Assessment Programme), other research organizations, and individual scientists to inform the prioritization of mitigation options with the best available science.

General steps to identify key Black carbon emission mitigation opportunities involve the following: 1) establishing the baseline of existing and forthcoming air quality policies and socio-economic trends such that both projected emission increases or decreases can be forecast in the absence of additional mitigation action over the next 10 to 20 years; 2) identifying from which sources and regions the residual opportunities lie to achieve further emission reductions; 3) estimating the costs of achieving such emission reductions; 4) applying a "climate filter" to these mitigation opportunities such that some approximation of the climate benefit—or, better still, the specific arctic climate benefit—of the mitigation actions can be assessed; and 5) assessing which policies (e.g., air quality policies targeting particulate matter) and programs (e.g., diesel engine retrofit initiatives) are best suited to deliver the desired mitigation actions, taking into account existing regulatory authorities, monitoring infrastructure and even political feasibility.

Regarding step 1, a key question is whether or not we have already identified all key Black carbon emission sources (current and projected) entering the Arctic, and whether any of the key emission inventory uncertainties, if further resolved, would change our understanding of the most important emission sources. Diesel engines, open biomass burning and marine shipping are known to be key emission sources. Regarding step 2, there is already ample information to identify what mitigation options and technologies are available to address the key sources. These include retrofitting diesel engines with particulate filters and altering the timing of existing springtime agricultural burning practices. Additional study is needed to

determine the impact of the potential sources (oil and gas flaring and industrial) and their most cost-effective mitigation measures.

Regarding step 4, a key question for the science community is whether simplified metrics and tools can be applied that would allow policy makers to gauge the arctic/ice melt benefits of reducing different emission sources (ideally taking into account the specific region and season). For example, some work is being conducted on regional GWPs for Black carbon, but there may be a way of calculating, say, an "arctic warming index" to help further prioritize key mitigation strategies. Ideally such an index would take into account co-emissions of non-absorbing aerosols.

Another set of questions faced by the task force is the extent to which sound recommendations can be made about addressing emissions that reach the Arctic but originate in non-Arctic Council countries. There is evidence that Asia is a significant source of Black carbon emissions reaching the Arctic.

At the time of this writing a formal schedule and work plan for the task force has not been developed but will be publically available.

The co-chairs of the task force are Benjamin DeAngelo of the U.S. Environmental Protection Agency and Håvard Toresen of the Norwegian Ministry of Environment.

Posters

Ny Ålesund Field Measurements

Variability of Albedo Using Unmanned Aerial Vehicles (VAUUAV)

http://transport.nilu.no/projects/vauuav
Wiley Bogren, wb@nilu.no

Purpose:

The 2009 VAUUAV field season took place over the month of May. The project was designed to investigate the impact of black carbon on snow albedo across varying spatial scales. In situ measurements and sampling characterize the local variation of albedo and reflectance at a ground site. Reflectance measurements from the UAV are to be validated against the ground measurements and used to extend the characterization across the 100+km flight path. At this scale, both ground and airborne measurements can be compared to satellite reflectance and albedo products, including MODIS data.

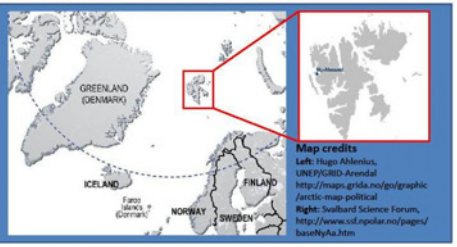

Map credits
Left: Hugo Ahlenius, UNEP/GRID-Arendal http://maps.grida.no/go/graphic/arctic-map-political
Right: Svalbard Science Forum, http://www.ssf.npolar.no/pages/baseNyAa.htm

Physical Sampling:

Black Carbon samples were collected on 13 separate days, from 5 locations including fast ice, glacial plateau, and pro-glacial tundra basin. Samples were collected from the top 5cm of the snowpack directly beneath the spectrometers.

The snowpack at optical sites was further characterized through quickpits, consisting of grain size and morphology as well as layer thickness observations over the top 50cm. The dataset consists of 88 quickpits, distributed throughout the Ny Ålesund area in the beginning of the campaign and focused on the Brøggerbreen pro-glacial basin towards the end of the month.

Above: A backlight snowpit beneath the TriOS sensors and a particularly icy, difficult-to-sample crust

Ocean Optics 'Jaz':

The Jaz spectrometer package consists of four probes, two each collecting at 277-880 nm and 340-1025nm. In most natural daylight conditions the Jaz is able to record measurements from all four probes as quickly as once per second. By comparison, the TriOS setup required 5 or 10 seconds between measurements from each sensor, but applied more of the necessary corrections and calibrations to the data before recording, saving substantial post-processing time and effort

60 measurements recorded at 1hz plotted on top of each other, representing one ground measurement interval with Ocean Optics Jaz spectrometer. Incoming radiation is plotted on the top row, reflected on the bottom. Red is the last plotted spectrum; variation over the measurement interval is represented in the colors beneath.

17 May Celebration:

The Norwegian National Holiday was a notable success for the VAUUAV crew in Ny Ålesund. The CryoWing UAV flew 119km in clear sky and relatively calm weather. The flight path crossed sections of both clean and dirty snow around Ny Ålesund, as well as open water and sea ice in the fjord. Additionally, concurrent reflectance measurements over the ground station were made at three elevations, and the ground station remained in place after the flight to establish comparison measurements with a near-nadir overpass of the TERRA satellite.

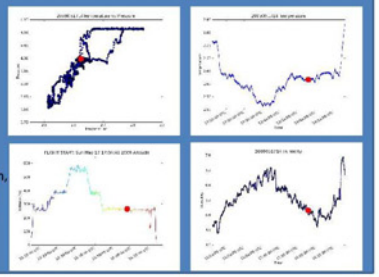

The ice/open water boundary in Kongsfjorden, identified in a MODIS satellite image, UAV's flight path, and a CryoWing aerial. This point in the flight is also marked on the altitude, temperature, humidity, and temperature vs pressure plots to the right. Colors correspond on the plots of altitude and flight path.

Ground-Based Measurements:

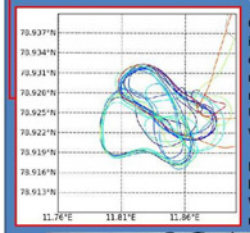

Overlapping reflectance measurements were made with three separate instrument packages. All collect incoming radiation through cosine-corrected diffusers. The trio of TriOS ground-based sensors collect reflected radiation as well through a diffuser, in addition to reflection values from a narrow aperture. The Ocean Optics 'Jaz' and the TriOS pair mounted on the UAV, by comparison, collect reflection values only through an aperture. This was chosen to help with processing data collected on a tilting platform.

Emphasis early in the season was placed on ground-based comparisons between the Ocean Optics spectrometer and the TriOS Ramses instruments. When flights began later in the month, emphasis was shifted to concurrent measurements between the ground and air based TriOS sensors.

From Top Left: Close up of flight tracks showing overpass pattern centered on ground station, TriOS ground station, and Jaz unit deployed

CryoWing UAV:

The CryoWing UAV, developed by the Northern Research Institute, flew more than 630km over a total 6 hours of flight, with light conditions varying from clear sky to heavy overcast. In addition to reflectance measurements, CryoWing collected temperature and humidity as well as a near-continuous series of aerial over surfaces including snow, open water, and late-season sea ice.

Flight Data:

The summary pages show a part of the wealth of information gathered during the CryoWing flights. Each of the five major flights provides around 100km of barometric, reflectance, and surface image profile data. The MODIS images shown are those acquired closest in time to the flights, and give an overview of both the weather and the opportunities for comparison to satellite reflectance products.

22 May Flight Summary

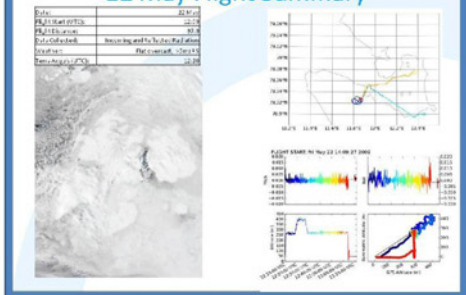

24 May Flight 2 Summary

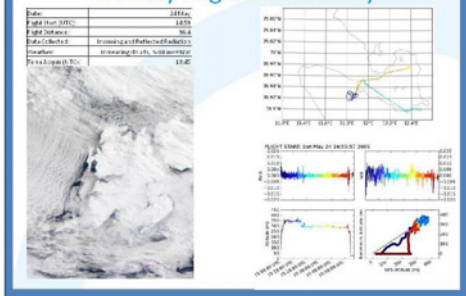

Acknowledgements:

The quality and variety of data brought back from this field season were made possible by the unstinting hard work of all the project partners in the field, including Dr. John Burkhart (NILU), Dr. Christina Pedersen (NP), Dr. Sebastian Gerland (NP), Dr. Johan Ström (NP) and Dr. Rune Storvold, Dr Stian Solbø, Andreas Tøllefsen from the Northern Research Institute.

Thanks also to the Norwegian Research Council for the funds supporting this project, and to the Norwegian Polar Institute for support of the field season.

Specific absorption coefficient, Seasonal variation of OC and EC: Observations from the Zeppelin station, Ny-Ålesund, Svalbard.

Johan Ström
Norwegian Polar Institute, Tromsø, Norway

Since the end of April 2006, weekly aerosol samples have been collected on quartz substrates for analysis of organic and elemental carbon. The analysis was conducted using the thermo-optical method by Sunset Labs. (NIOSH protocol).

Since March 2002, hourly observations of aerosol light absorption has been conducted using a custom built PSAP-type instrument. Data from a TSI-3563 Nephelometer was used to correct for light scattering aerosols.

For the overlapping time period, weekly averages were calculated from the hourly data. By combining the two sets of information, a specific absorption coefficient can be derived. With this values it is possible to relate the light absorption measurements to an EC or BC (Black Carbon) concentration in air.

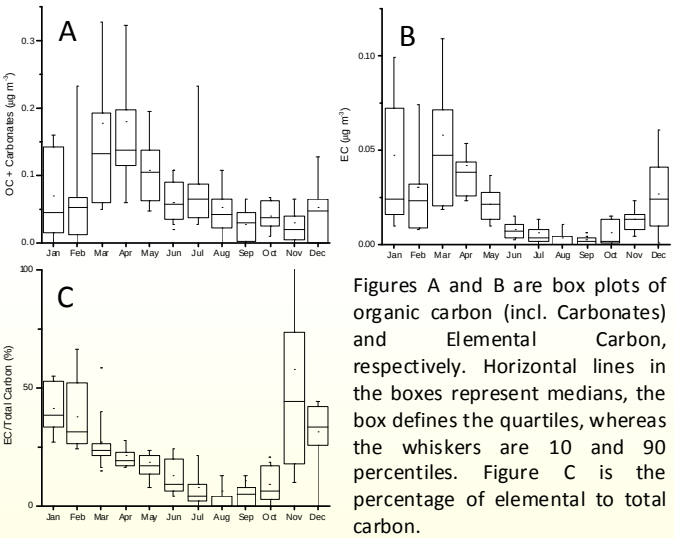

Figures A and B are box plots of organic carbon (incl. Carbonates) and Elemental Carbon, respectively. Horizontal lines in the boxes represent medians, the box defines the quartiles, whereas the whiskers are 10 and 90 percentiles. Figure C is the percentage of elemental to total carbon.

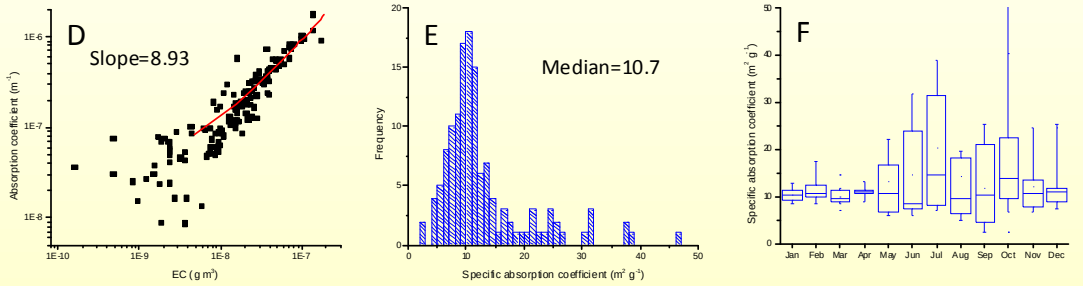

Figure D is a scatter plot of the EC concentrations and light absorption coefficient. The slope is 8.93, which would be the value of the specific absorption coefficient. Figure E is a histogram of this parameter, calculated for each pair of data. The median is 10.7. Figure F is a presentation of how this value change over the year. It is difficult to see a clear trend in the median value as such, although there is a skewness toward higher values in the summer. The summer period is a little problematic due to very low values and larger uncertainties as a result of this.

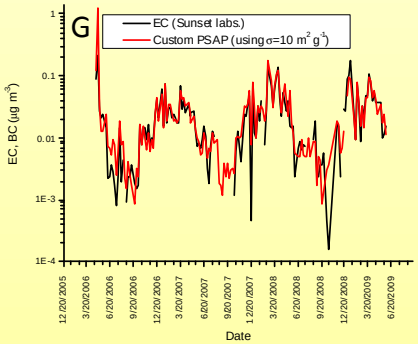

Figure G presents the time series of weekly EC samples collected on quarts filters and analyzed with a thermo-optical method, and the weekly averaged hourly PSAP data using a specific absorption coefficient of 10 $m^2 g^{-1}$).

Concluding remarks

- In winter, EC often contributes 1/3 or even more of the total carbon in aerosols.
- Using a specific absorption coefficient of 10 $m^2 g^{-1}$, brings a good agreement between EC measured by a thermo-optical method and BC measured by an optical method.
- Although higher coefficients were observed in the summer, it is difficult to determine any seasonal trend due to the low ambient concentrations of EC during summer.

Thanks to ITM, Stockholm University for providing the data.

Contact: johan.strom@npolar.no

Summary of working group I: Models

Compiled by Dorothy Koch

1. Organization of old and new arctic BC data;
    a. data access.

    These might be used to compare with AeroCom 2007 simulations
2. Establishment of long-term BC monitoring stations of BC in air and snow. Preferably in "optimal" locations in terms of impact and model uncertainty
    a. East Arctic
    b. Southeast Asia
3. Removal process constraints:
    a. scavenging of BC by snow/ice, rain
    b. dry vs wet deposition
4. Aerosol microphysical information (mixing state of arctic BC)
5. Biomass burning vs fossil fuel BC in more locations.14C analysis (co-located with Hegg measurements?)
6. Impacts of BC on snow grain size, experimental analysis?
7. Ice core records and other long-term time series

The figure (from Koch et al., 2009) below illustrates variability among the global models in how they simulate annual mean surface concentrations of BC in the air. At high northern latitudes the standard deviation is similar or larger that the average of the 14 models participating in the AEROCOM experiment

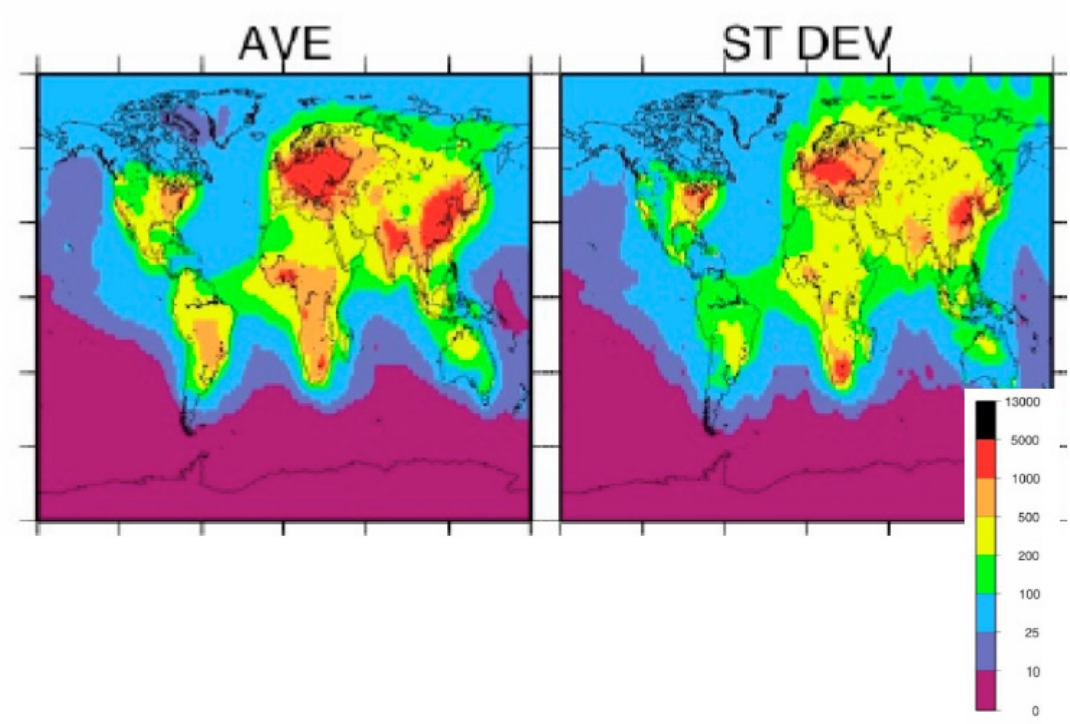

AeroCom models' annual mean BC surface concentrations (ngm^{-3}). First panel shows the average, second panel shows standard deviation of models. From Koch et al. (2009)

Summary of working group II: Measurements

Compiled by Stephen G. Warren and Sarah Doherty

What is measured?

Three methods are now used to measure Black carbon (BC) or Elemental carbon (EC) in snow and ice:
(1) Photometry of filters, which measures mass of BC
(2) Thermo-optical method, giving mass of EC
(3) Single Particle Soot Photometer (SP2) which give the mass of individual particles of EC of size <500 nm; thereby also yielding a size distribution.

BC/EC content of snow samples have been measured using the first two methods, with plans to also measure snow samples using the SP2 method. EC in ice cores has been measured using only the SP2 method.

The photometric measurement method also allows for determination of the fraction of light absorption due to non-BC species, using the spectral "fingerprint" of pure soot to separate light absorption by soot vs. by other species (e.g. organic or "brown" carbon and dust).

In addition to quantifying EC/BC, chemical analysis has been done on ice cores and on some snow samples in order to elucidate the aerosol sources via chemical fingerprints.

What has been found?

Some results so far:
(1) Springtime snow in Canada and the Arctic Ocean now has less BC than in 1983–4.
(2) For the samples analyzed to date the major source of BC in Arctic Alaska, Canada, Greenland, and Russia is biomass burning.
(3) EC mass as measured using the thermo-optical method is a about a factor of 2 lower than BC mass derived from filter photometry.
(4) EC/BC in air at arctic sites has a strong seasonal cycle
(5) Measurement of EC/BC is snow is not only dependent on the concentrations in the air, but very much on the amount of precipitation

Recommendations regarding methods of measurement

Reports of results from each BC measurement technique should include
(a) a clear definition of what is measured;
(b) sources of uncertainty,
(c) sources of bias (e.g., filter efficiency), and
(d) assumptions used.

The participants agreed to collate this information for the three measurement methods used.

Intercomparisons of methods should be done on
(a) co-located samples of natural snow
(b) reference standards (commercial soots).

An important question will be whether the differences exceed the defined uncertainties.

There appear to be mixed results as to the efficiency of filter-catch for the filters used in the photometric (0.4μm nuclepore) and thermo-optical (quartz fiber) measurements. More extensive tests of filter efficiency for lab-generated and field aerosol should be made to examine a possible bias to larger sizes and particular sources of BC.

Ice cores analyzed for EC have been drilled at elevations in the mid-troposphere. Values of EC in ice cores should be related to EC in snow samples at nearby low-elevation sites, in order to examine the effect of altitude on EC deposition rates.

How can measurements be useful to models, and vice versa?

We need to determine what is driving the seasonal cycles of BC and what determines the time-evolution of BC at different levels in the snowpack. Measurements of snow EC/BC that are accompanied by chemical analysis and backtrajectory analysis can be used to help determine the source of the EC/BC.

Comparisons of models with measurements of BC in snow can help test model representation of

- Geographical distribution in modern climate
- Seasonal cycle and long-term changes (from ice cores)
- Source types

Recommendations for measurements that can provide tests or constraints to modeling

a.) Some measurements indicate that EC/BE may consolidate at the snow surface when there is sublimation and/or when snow melts. Noting that the top model layer is ~2 cm thick and that the second model layer is 2–3cm thick, these should be the top two layers of field samples while measuring vertical profiles under two conditions:

- Monitor vertical profiles of BC/EC in snow throughout the winter and spring at a few sites that experience sublimation but no melt during winter.
- Monitor the vertical redistribution of BC during snowmelt. Corresponding chemical analyses will be valuable to distinguish migration of BC from new dry-deposition. Snow depth during winter-spring is monitored at Pallas (Finland); this would be a good site for monitoring snowmelt because the snow is cold in winter and there is normally no melting until late spring.

b.) Sample snow in locations where models predict the highest concentrations of BC: southern Finland and neighboring far-western Russia, 60–63°N. There are currently no measurements from these areas of which we are aware.

c.) Continue long-term atmospheric measurements of BC at arctic monitoring sites (Ny-Ålesund, Alert, Barrow), to monitor inter-annual variations and trends.

d.) Measure EC in ice cores to get the history of EC, and associated chemical indicators of sources, over several centuries at high-altitude locations.

e.) Collect samples of individual snowfall events. Apply trajectory analysis and chemical analysis to identify sources. These would best be done at sites that are already instrumented

for atmospheric measurements (Zeppelin, Pallas, Abisko, Summit), or that will be instrumented as part of the Arctic Observing Network.

f.) Design experiments to measure directly the effect of BC on snow albedo. This is being done in natural snowpacks by Pedersen et al., in artificial snowpacks by Brandt and Warren, and in the laboratory by Zender et al. Sources of error in albedo measurements (Grenfell et al., 1994 JGR) and the strong dependence of albedo on grain size need to be taken into account.

g.) Vertical profiles of EC in the troposphere from SP2 on aircraft would be useful to assist the modeling of transport and deposition.

h.) In order to make diverse measurements by different groups useful to modelers, measurement protocols for snow sampling should be established for:

(1) new snow
(2) melting snow
(3) profiles
(4) snow-water sampling for chemical analysis

Recommendations for models

Evaluate sensitivity of BC radiative forcing to:

a.) Vertical resolution in the snowpack (i.e. of grain size and BC/EC content)
b.) Using a probability density function (pdf) of snow depth within a gridbox
c.) Snow patchiness / distribution within a gridbox
d.) Snow grain-size prediction
e.) Screening of snow by vegetation
f.) Spectral interaction of clouds and snow for solar radiation

Neglected topics

The group did not discuss remote sensing of the BC content of snow. The only speaker who mentioned remote sensing (R. Solberg) was skeptical that remote sensing of BC in snow would be possible due to the very small changes in albedo (generally <0.02) and high sensitivity to, e.g., surface slope and spatial variations in terrain and snowdepth within the sensor field of view, among other factors.